# Stochastic wave finite element quadratic formulation for periodic media: 1D and 2D

R. P. Singh, C. Droz, Mohamed Ichchou, F. Franco, O. Bareille, S. de Rosa

# Stochastic wave finite element quadratic formulation for periodic media: 1D and 2D

R.P. Singh[a,b], C. Droz[a], M. Ichchou[a], F. Franco[b], O. Bareille[a], S. De Rosa[b]

[a] *Vibroacoustics & Complex Media Research Group, LTDS - CNRS UMR 5513, Ecole Centrale de Lyon, Ecully, France*
[b] *PASTA Lab, Department of Industrial Engineering, University of Naples Federico II, Via Claudio 21, 80125 Napoli, Italy*

**Abstract**

Periodic structures have properties of controlling mechanical waves. These solutions are used in aircraft, trains, submarines, space structures where high level of robustness has to be ensured in presence of uncertainty in the numerical models. The paper presents a stochastic formulation for the Bloch analysis of periodic structures, based on the quadratic 1D and 2D forms of the Wave Finite Element method. In 1D case, numerical examples of periodic rod and metamaterial rod systems are considered; for the 2D case, homogeneous and periodic plates considered. In both cases, the effect of uncertainties on wavenumber variation is studied. The accuracy and performance of the developed method is compared with Monte Carlo simulation (MCS) results. It is found that the uncertainties affects the wavenumber scattering. Maximum variation of wavenumber occurs at the band gap edge frequencies and trends are increasing in higher frequency. In terms of computational cost, the presented formulation offers computational advantages over MCS. The computational cost savings can be a good point for the optimization and reliability study under uncertainties of complex structures.

*Keywords:* Periodic media, uncertainties, band gap, stochastic approach, wavenumber

**Highlights**

- A stochastic quadratic eigenvalue formulation for the periodic media is presented.
- The longitudinal and flexural waves in the 1D and 2D periodic media are simulated.
- In the case of flexural wave, only out of plane flexural wave are generated.
- The formulation offers computational advantages over the Monte Carlo simulation.

*Email address:* ravipratap-singh@ec-lyon.fr, ravipratap.singh@unina.it (R.P. Singh)

**Contents**

## 1. Introduction

The vibroacoustic performance and dynamics of the structure are essential subjects in aeronautics, transport, energy, and space. The structures having periodic properties or repeating patterns show a peculiar feature known as band gaps. Band gaps are defined as frequency intervals where both sound and vibration are forbidden from propagating. Application of this concept can be used [1] for vibration reduction, acoustic blocking, acoustic channelling, and acoustic cloaking. The periodic models are used for the vibration attenuation and control in dynamic [2], [3] and acoustic reduction in railway tracks [4]. Different methods developed in the literature for modelling of periodic structures, such as plane wave expansion method [5], finite difference time domain method [6], multiple scattering method [7], transfer matrix (TM) method [3], wave finite element method (WFEM) [8], and differential quadrature method [9].

The design of periodic media is generally based on deterministic models without considering the effect of inherent uncertainties existing in these media. In general, the design is aimed at controlling as much as possible the mechanical waves; however, inherent uncertainties may affect their characteristics. The uncertainties, in terms of material properties and geometrical parameters, are mostly exhibited in both manufacturing and assembly processes. To address this unavoidable actuality, the effects of uncertainties need to be considered when analysing frequency band structures (pass and stop bands).

Generally, the stochastic characteristics of the periodic media can be determined by studying the design parameter uncertainties, which are often modelled by random variables with consideration for spatial variability of the material and geometrical properties. The uncertainties in the material properties scatter the wave in comparison with the deterministic prediction.

Miles [10] proposed an asymptotic solution for the one-dimensional wave propagation in heterogeneous elastic with the variation of Young's modulus and density. The application of the Wentzel-Kramers-Brillouin (WKB) approximation in the structural dynamics for the inhomogeneous system is introduced by Steele [11]. Manohar et al. [12] studied the randomness in the wave propagation in waveguides using spectral element analysis. Langley [13] developed a method which enables the average value of the inverse squared transmission coefficient to calculated for the one dimensional near periodic structure. Arenas [14] studied an incident plane sound wave travelling along a rigid duct where the impedance of a particular horn obtained using the WKB approximation. Sarkar et al. [15] presented a parametric stochastic finite element approach based on polynomial expansion in conjunction with proper orthogonal decomposition method and dynamic element method for the mid-frequency vibration analysis. Ichchou et al. [16] proposed a numerical approach using the WFEM based on the TM considering spatially homogeneous variability in waveguides using first-order perturbation theory for the random guided viscoelastic media in the broad frequency range. Ben Souf et al. [17] presented hybrid WFEM and stochastic wave finite element method (SWFEM) to develop a diffusion matrix of the coupling structure. Ben Souf et al. [18] studied the forced response of the random viscoelastic media subject to time-harmonic loading by hybridisation of the deterministic WFEM and a parametric probabilistic

approach. Ben souf et al. [19] studied uncertainty propagation in the forced response of the periodic coupled structure by hybridisation of WFEM and generalised polynomial chaos expansion. In addition they investigated the modal uncertainties effect on the random dynamic response of periodic structures [20]. Fabro et al. [21] investigated force response of the finite waveguide undergoing longitudinal and flexural motion using WKB approximation for random material and geometrical properties. Also derived approximation with considering waveguide with piecewise constant material variability to mitigate the effect of the internal reflections which occur due to any local changes in the material or geometrical properties and verified with the experimental investigation.

Recently in the 1D periodic media, Mencik et al. [22] presented a method to compute the forced response of the periodic structures with many perturbed substructures. Fabro et al. [23] studied the robustness of the band gap by employing wave finite element transfer matrix (WFEM TM) with WKB and Karhunen-Loeve expansion for the undulated beam with and without resonators. Li et al. [24] presented a study considering the material and geometrical uncertainty on the band structures of an undulated beam with the periodically arched shape. The band gap calculated using finite element method (FEM) and uncertainty propagated using the interval analysis based on the Taylor series expansion. Bouchoucha et al. [25] proposed the second order perturbation of the one-dimensional SWFEM method proposed by Ichchou et al. [16]. Ma et at. [26] studied the dynamic response of the uncertainty frame structure and proposed the travelling wave method integrated with interval method considering uncertainty in the geometric dimension and external load. Fabro et al. [27] proposed a method to extend the applicability of WKB expansion approach using finite element method. The latest development by Zhao et al. [28] studied symplectic eigenvalue problem of the random symplectic matrix employing the Rayleigh quotient method for the study of 1D chain with homogenous randomness.

In 2D periodic media with uncertainty, Ben Souf et al. [29] studied the effect of uncertain parameters on sound transmission loss for the composite panels using the generalised polynomial chaos expansion applied with a high level of uncertainty. Xie et al. [30] investigated the topology optimisation of 2D Phononic crystals (PnCs) with uncertainties and proposed surrogate model-based heuristic algorithm. The band diagram computed with the plane wave expansion method and interval model is introduced to handle the uncertainties based on Monte Carlo simulation (MCS). Zakian et al. [31] proposed a stochastic spectral finite element method for the wave propagation in random media in the 2D plate in the time domain.

The literature reveals that the effects of uncertainty in the material properties, geometry, loading condition and model, play a significant role in altering the state of the wave. The motivation of present work is in the development of a numerical tool for the stochastic modelling of 1D and 2D periodic media for the weak level of uncertainties at reduced computation cost. The choice of spectral problem is motivated by the fact that it offers [32]: a dynamic condensation of the element inner degree of freedom (DOF) to reduce computational DOFs; it allows to compute group velocity for finding wave directivity; and provides information about imaginary part of the propagative wave which enable computation of forced response from wave based method. This paper focused on employing first-order perturbation theory to predict the wave dispersion using spectral problem. The formulation proposes a straightforward

approach for the stochastic wave modelling in the periodic structure. The main advantage of the formulation is that, commercial finite element (FE) packages, and FE routines can be used for meshing capabilities during the modelling of the real structure. In this paper, the SWFEM based on transfer matrix [16] is also extended to 1D periodic media cases. The innovative contribution is in the development of the stochastic formulation for Bloch analysis of periodic structures, based on the quadratic 1D and 2D forms of the Wave Finite Element method. The results of the stochastic formulation are compared to those obtained with analytical sampling and MCS results.

The paper is organized as follows: Section 2 presents the formulation for the 1D periodic media. Section 3 provides a formulation for the 2D periodic media. In Section 4, the numerical results and validation are presented. The elapsed time comparison is presented in Section 5. Finally, Section 6 provides the concluding remarks.

## 2. SWFEM quadratic formulation: 1D periodic media

In the deterministic case, dispersion curve extracted by spectral analysis. The use of a state space representation is an interesting alternative to the spectral analysis. However, the numerical ill-conditioning may occur when a large number of the unit cells are involved in the periodic system model using the TM method [33].

To overcome this shortcoming for the stochastic modelling, the stochastic quadratic formulation is presented in this section for the 1D periodic media. Also the formulation is adopted for the metamaterial system.

### *2.1. SWFEM quadratic formulation*

Consider a one-dimensional periodic system, as shown in Fig.1. One dimensional periodic structures are obtained by formulating the unit cell and then repeating in the propagation direction. Then, the study of this structure is converted into a study of unit cell based on the Floquet-Bloch theorem [34].

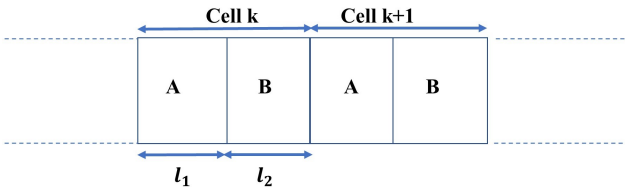


Figure 1: Schematic representation of the periodic structure

The variables are displacements as $q$ and forces as $F$. Introducing the dynamic stiffness matrix $(D) = -\omega^2 M + K(1 + i\eta)$, where $K$ is the stiffness matrix, $M$ is the mass matrix, $\eta$ is the loss factor and $i$ is the unit imaginary number. The node on boundary of the periodic structure is denoted as on left boundary ($L$), right boundary ($R$) and remaining/internal nodes ($I$). The displacement DOF $q$ are partitioned into the left ($q_L$) and right ($q_R$). Similarly, forces are partitioned into the left ($F_L$) and right ($F_R$). Firstly, the deterministic form of the quadratic eigenvalue

problem is obtained. The dynamic of the global waveguide can be expanded on wave solution as follows

$$q_R = \mu q_L \text{ and } F_R = -\mu F_L \tag{1}$$

where $\mu$ is the propagation constant. Floquet-Bloch condition applied to the dynamic equation, leads to the classic quadratic eigenvalue problem [35] in terms of propagation constant

$$\left(D_{RL} + \mu_i I_{2n} \left(D_{LL} + D_{RR}\right) + \mu_i^2 I_{2n} D_{LR}\right)\left(\Phi_q\right)_i = 0 \tag{2}$$

where $i = 1...2n$, $n$ is the cross sectional DOFs, $D_{LL}$, $D_{RL}$, $D_{RR}$ and $D_{LR}$ are the element of the dynamic stiffness matrix. The wave mode of the global system is $\left((\mu_i, (\Phi_q)_i)\right)_{i=1...2n}$. Based on the quadratic eigenvalue form, to accommodate the uncertainties effects, the stochastic equation of motion can be expressed in the form

$$\widetilde{D}\,\widetilde{q} = \widetilde{F} \tag{3}$$

where symbol $\widetilde{(.)}$ denotes the stochastic entity. The Eq. (3) can be partitioned as follows

$$\begin{pmatrix} \widetilde{D}_{LL} & \widetilde{D}_{LR} \\ \widetilde{D}_{RL} & \widetilde{D}_{RR} \end{pmatrix} \begin{pmatrix} \widetilde{q}_L^k \\ \widetilde{q}_R^k \end{pmatrix} = \begin{pmatrix} \widetilde{F}_L^k \\ \widetilde{F}_R^k \end{pmatrix} \tag{4}$$

Using the dynamic stiffness matrix symmetry, stochastic quadratic eigenvalue problem can be written as

$$\left(\widetilde{D}_{RL} + \widetilde{\mu}_i I_{2n} (\widetilde{D}_{LL} + \widetilde{D}_{RR}) + \widetilde{\mu}_i^2 I_{2n} \widetilde{D}_{LR}\right)\left(\widetilde{\Phi}_q\right)_i = 0 \tag{5}$$

Using polynomial chaos projection of the variables in the Eq. (5), we can also extract their mean value $\overline{(.)}$ and standard deviation ($\sigma$). The explicit expression for the standard deviation of the eigenvalues and eigenvectors are derived in Appendix A. The explicit expression for the standard deviation of the eigenvalues ($\sigma_{\mu_i}$) is

$$\begin{aligned}
\sigma_{\mu_i} = \left(\overline{\Phi}_q\right)_i^T & \left[\sigma_{D_{RL}}^T + \overline{\mu}_i I_{2n} \left(\sigma_{D_{LL}} + \sigma_{D_{RR}}\right)^T + \overline{\mu}_i^2 I_{2n} \sigma_{D_{LR}}^T\right]\left[\overline{D}_{RL} + \overline{\mu}_i I_{2n} (\overline{D}_{LL} + \overline{D}_{RR}) + \overline{\mu}_i^2 I_{2n} \overline{D}_{LR}\right]^{-1} \\
& \left[\overline{D}_{RL} + \overline{\mu}_i{}^{-1} I_{2n} (\overline{D}_{LL} + \overline{D}_{RR}) + \overline{\mu}_i{}^{-2} I_{2n} \overline{D}_{LR}\right] - \left(\overline{\Phi}_q\right)_i^T \left[\sigma_{D_{RL}} + \overline{\mu}_i{}^{-1} I_{2n} \left(\sigma_{D_{LL}} + \sigma_{D_{RR}}\right) + \overline{\mu}_i{}^{-2} I_{2n} \sigma_{D_{LR}}\right] \\
& \left[\left(\overline{\Phi}_q\right)_i^T \left[-(\overline{D}_{LL} + \overline{D}_{RR})^T - 2\overline{\mu}_i I_{2n} \overline{D}_{LR}^T\right]\left[\overline{D}_{RL} + \overline{\mu}_i I_{2n} (\overline{D}_{LL} + \overline{D}_{RR}) + \overline{\mu}_i^2 I_{2n} \overline{D}_{LR}\right]^{-1}\right. \\
& \left.\left[\overline{D}_{RL} + \overline{\mu}_i{}^{-1} I_{2n} (\overline{D}_{LL} + \overline{D}_{RR}) + \overline{\mu}_i{}^{-2} I_{2n} \overline{D}_{LR}\right] - \left(\overline{\Phi}_q\right)_i^T \left[\overline{\mu}_i{}^{-2} I_{2n} (\overline{D}_{LL} + \overline{D}_{RR}) + 2\overline{\mu}_i{}^{-3} I_{2n} \overline{D}_{LR}\right]\right]^{-1}
\end{aligned} \tag{6}$$

Explicit expression for the standard deviation of the eigenvectors ($\sigma_{(\Phi_q)_i}$) is

$$\begin{aligned}
\sigma_{(\Phi_q)_i} = & -\left[\overline{D}_{RL} + \overline{\mu}_i I_{2n} (\overline{D}_{LL} + \overline{D}_{RR}) + \overline{\mu}_i^2 I_{2n} \overline{D}_{LR}\right]^{-1} \\
& \left[\sigma_{D_{RL}} + \sigma_{\mu_i I_{2n}} (\overline{D}_{LL} + \overline{D}_{RR}) + \overline{\mu}_i I_{2n} \left(\sigma_{D_{LL}} + \sigma_{D_{RR}}\right) + 2\overline{\mu}_i \sigma_{\mu_i} I_{2n} \overline{D}_{LR} + \overline{\mu}_i^2 I_{2n} \sigma_{D_{LR}}\right]\left(\overline{\Phi}_q\right)_i
\end{aligned} \tag{7}$$

Eq. (6) and Eq. (7) are the the explicit expressions for the statistical characterization of the wavenumber using deterministic eigenvalue solutions in the periodic media.

### 2.2. Internal nodes

If the formulation requires the dynamic condensation of the inner DOFs at each frequency step, the standard deviation of the condensed dynamic stiffness matrix has to be evaluated. Having internal DOFs,($I$) as shown in Fig. 2,

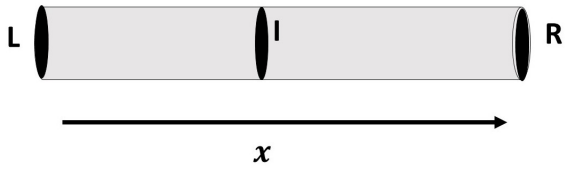


Figure 2: Rod element with internal node

the DOFs are partitioned into the left boundary DOFs ($D_L$), right boundary DOFs ($D_R$) and internal DOFs ($D_I$). Introducing uncertainties in the parameters, the stochastic dynamic stiffness matrix has the following form

$$\widetilde{D} = \begin{bmatrix} \widetilde{\widehat{D}}_{LL} & \widetilde{\widehat{D}}_{LI} & \widetilde{\widehat{D}}_{LR} \\ \widetilde{\widehat{D}}_{IL} & \widetilde{\widehat{D}}_{II} & \widetilde{\widehat{D}}_{IR} \\ \widetilde{\widehat{D}}_{RL} & \widetilde{\widehat{D}}_{RI} & \widetilde{\widehat{D}}_{RR} \end{bmatrix} \tag{8}$$

where symbol $\widetilde{\widehat{(.)}}$ represents the stochastic entity from the original dynamic stiffness matrix. The dynamic condensation and the zero order expansion of the above equation leads to

$$\overline{\mathrm{D}} = \begin{bmatrix} \overline{D}_{LL} & \overline{D}_{LR} \\ \overline{D}_{RL} & \overline{D}_{RR} \end{bmatrix}$$

$$\overline{\mathrm{D}} = \begin{bmatrix} \overline{\widehat{D}}_{LL} - \overline{\widehat{D}}_{LI}\overline{\widehat{D}}_{II}^{-1}\overline{\widehat{D}}_{IL} & \overline{\widehat{D}}_{LR} - \overline{\widehat{D}}_{LI}\overline{\widehat{D}}_{II}^{-1}\overline{\widehat{D}}_{IR} \\ \overline{\widehat{D}}_{RL} - \overline{\widehat{D}}_{RI}\overline{\widehat{D}}_{II}^{-1}\overline{\widehat{D}}_{IL} & \overline{\widehat{D}}_{RR} - \overline{\widehat{D}}_{RI}\overline{\widehat{D}}_{II}^{-1}\overline{\widehat{D}}_{IR} \end{bmatrix} \tag{9}$$

The first order expansion leads to the standard deviation of the condensed dynamic stiffness matrix (detailed derivation in Appendix B)

$$\sigma_D = \begin{bmatrix} \sigma_{\widehat{D}_{LL}} & \sigma_{\widehat{D}_{LR}} \\ \sigma_{\widehat{D}_{RL}} & \sigma_{\widehat{D}_{RR}} \end{bmatrix} - \begin{bmatrix} \overline{\widehat{D}}_{LI} & \sigma_{\widehat{D}_{LI}} \\ \overline{\widehat{D}}_{RI} & \sigma_{\widehat{D}_{RI}} \end{bmatrix} \begin{bmatrix} \overline{\widehat{D}}_{II}^{-1} & -\overline{\widehat{D}}_{II}^{-1}\sigma_{\widehat{D}_{II}}\overline{\widehat{D}}_{II}^{-1} \\ 0 & \overline{\widehat{D}}_{II}^{-1} \end{bmatrix} \begin{bmatrix} \sigma_{\widehat{D}_{IL}} & \sigma_{\widehat{D}_{IR}} \\ \overline{\widehat{D}}_{IL} & \overline{\widehat{D}}_{IR} \end{bmatrix} \tag{10}$$

where symbol $\overline{\widehat{(.)}}$ represents the mean value from the original dynamic stiffness matrix. The Eq. (10) is used for accommodating contribution of standard deviation of the condensed DOFs on the boundary DOFs.

### 2.3. Attached resonators

For the low-frequency range, the band gaps can be achieved by mounting the periodically local resonators. The locally resonance (LR) metamaterial-based rod system consists of a uniform rod and periodically attached spring ($k_i$)

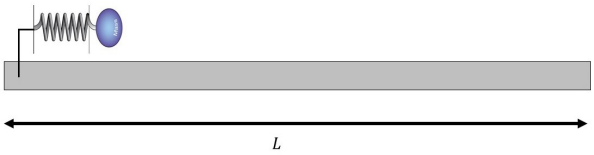


Figure 3: Unit cell with local resonator

and mass ($m_i$). The number of springs and masses in resonator can be chosen based on targeted band gap characteristics as per design of the metamatrial rod [36]. The unit cell of the LR rod shown in Fig.3. Where dynamic stiffness matrix ($D_0$) of the resonator at the attachment point can be written as

$$D_0 = k - \left(k^2 / \left(k - \omega^2 m\right)\right) \tag{11}$$

Once the dynamic stiffness matrix for the LR is obtained, then it needs to be attached to the unit cell of the host structures. The dynamic stiffness matrix of the LR rod obtained as

$$D = \begin{bmatrix} D_{LL} & D_{LR} \\ D_{RL} & D_{RR} \end{bmatrix} = \begin{bmatrix} D_{LL} + D_0 & D_{LR} \\ D_{RL} & D_{RR} \end{bmatrix} \tag{12}$$

In the host structure, the stochastic equation of motion can be expressed as

$$\begin{pmatrix} \widetilde{D}_{LL} & \widetilde{D}_{LR} \\ \widetilde{D}_{RL} & \widetilde{D}_{RR} \end{pmatrix} \begin{pmatrix} \widetilde{q}_L^k \\ \widetilde{q}_R^k \end{pmatrix} = \begin{pmatrix} \widetilde{F}_L^k \\ \widetilde{F}_R^k \end{pmatrix} \tag{13}$$

Above expression is similar to the stochastic equation of motion express in Eq. (4). The stochastic wavenumber characterization can be obtained by using explicit Eq. (6), Eq. (7) which are discussed in the previous subsection 2.1.

## 3. SWFEM quadratic formulation: 2D periodic media

### *3.1. Four noded rectangular element*

Considering an infinite thin plate lying in the $(x, y)$ plane and its unit cell is shown in Fig. 4. The unit cell is divided into four corner nodes. The unit cell DOFs ($q$) are divided into four corner nodal DOFs, $q_1, q_2, q_3$ and $q_4$.

The vector of nodal DOFs are given by $q = \left[q_1^T, q_2^T, q_3^T, q_4^T\right]^T$, similarly, the vector of nodal forces are given by $f = \left[f_1^T, f_2^T, f_3^T, f_4^T\right]^T$. Where $T$ denotes the transpose.

The time-harmonic equation of motion of the unit cell can be written as

$$\left(K - \omega^2 M\right) q = f \tag{14}$$

where $K$ is the stiffness matrices, $M$ is the mass matrices, $\omega$ is the circular frequency, $f$ is the nodal forces vector and $q$ is the nodal displacements vector. This equation is used to form the spectral problem involving wavenumber $k_x, k_y$ and frequency $\omega$. The dynamic stiffness matrix can be expressed as $D = K - \omega^2 M$.

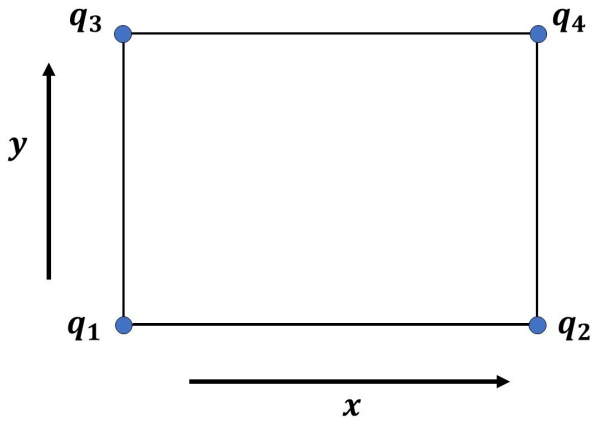


Figure 4: Rectangular plate element

Here introducing the periodic structure theory for the unit cell and considering a time-harmonic response ([37]) the deterministic harmonic equation of motion can be expressed as

$$\left(K^*\left(\lambda_x,\lambda_y\right)-\omega^2 M^*\left(\lambda_x,\lambda_y\right)\right)q_1=0 \tag{15}$$

where $K^*=\Lambda_L K\Lambda_R$ and $M^*=\Lambda_L M\Lambda_R$ are the reduced stiffness and mass matrices. $\lambda_x$ and $\lambda_y$ are the propagation constants in $x$ and $y$ direction respectively. $\Lambda_L$ and $\Lambda_L$ are matrices which contains the propagation constants from the periodicity conditions.

$$\Lambda_L=\begin{bmatrix} I & \lambda_x^{-1}I & \lambda_y^{-1}I & \lambda_x^{-1}\lambda_y^{-1}I \end{bmatrix}$$

$$\Lambda_R=\begin{Bmatrix} I \\ \lambda_x I \\ \lambda_y I \\ \lambda_x\lambda_y I \end{Bmatrix} \tag{16}$$

where $I$ is the identity matrix.

The eigenvalue problem of Eq.( 15) can be expressed as

$$D^*\left(\omega,\lambda_x,\lambda_y\right)q_1=0 \tag{17}$$

where $D^*\left(\omega,\lambda_x,\lambda_y\right)$ is the reduced dynamic stiffness matrix. For the shake of clarity the reduced dynamic stiffness matrix is now represented as $D$. If reduced dynamic stiffness matrix partitioned as

$$D=\begin{bmatrix} D_{11} & D_{12} & D_{13} & D_{14} \\ D_{21} & D_{22} & D_{23} & D_{24} \\ D_{31} & D_{32} & D_{33} & D_{34} \\ D_{41} & D_{42} & D_{43} & D_{44} \end{bmatrix} \tag{18}$$

Then the eigenvalue problem in Eq. (17) can be written in the following form

$$\Big[(D_{11}+D_{22}+D_{33}+D_{44})+(D_{12}+D_{34})\lambda_x+(D_{21}+D_{43})\lambda_x^{-1}+(D_{13}+D_{24})\lambda_y+(D_{31}+D_{42})\lambda_y^{-1} \\ +D_{14}\lambda_x\lambda_y+D_{41}\lambda_x^{-1}\lambda_y^{-1}+D_{32}\lambda_x\lambda_y^{-1}+D_{23}\lambda_x^{-1}\lambda_y)\Big]q_1=0 \quad (19)$$

The solution of Eq. (17) in the case where frequency and one wavenumber in $x$ or $y$ direction are known, the eigenvalue form becomes a quadratic eigenvalue problem. Then the nonlinear Eq. (19) can be reduced to quadratic eigenproblem in $\lambda_x$ form when $\lambda_x$ is unknown and $(\omega, \lambda_y)$ are given

$$\Big[(D_{21}+D_{43}+D_{41}\lambda_y^{-1}+D_{23}\lambda_y)+\mu_i(D_{11}+D_{22}+D_{33}+D_{44}+(D_{31}+D_{42})\lambda_y^{-1}+(D_{13}+D_{24})\lambda_y) \\ +\mu_i^2(D_{12}+D_{34}+D_{32}\lambda_y^{-1}+D_{14}\lambda_y)\,]\left(\Phi_q\right)_i=0 \quad (20)$$

For the stochastic modelling, assume that uncertainties are spatially homogeneous to guarantees the periodicity assumption to be respected in the stochastic case. The stochastic equation of motion can be expressed as

$$\widetilde{D}\left(\omega,\lambda_x,\lambda_y\right)q_1=0 \quad (21)$$

where stochastic dynamic stiffness matrix $(\widetilde{D})$ has the form $\widetilde{D}=(\overline{D}+\sigma_D\varepsilon)$. $(\varepsilon)$ is Gaussian variable centred and reduced. Above Eq. (21) extends Eq. (17) to the stochastic case. Then the stochastic spectral problem is expressed as

$$\Big[(\widetilde{D}_{21}+\widetilde{D}_{43}+\widetilde{D}_{41}\lambda_y^{-1}+\widetilde{D}_{23}\lambda_y)+\widetilde{\mu}_i I_{2n}(\widetilde{D}_{11}+\widetilde{D}_{22}+\widetilde{D}_{33}+\widetilde{D}_{44}+(\widetilde{D}_{31}+\widetilde{D}_{42})\lambda_y^{-1}+(\widetilde{D}_{13}+\widetilde{D}_{24})\lambda_y) \\ +\widetilde{\mu}_i^2 I_{2n}(\widetilde{D}_{12}+\widetilde{D}_{34}+\widetilde{D}_{32}\lambda_y^{-1}+\widetilde{D}_{14}\lambda_y)\Big]\left(\widetilde{\Phi}_q\right)_i=0 \quad (22)$$

where $\left(\widetilde{\mu}_i,\widetilde{\phi}_i\right)_{i=1\ldots2n}$ are the stochastic waveguide propagation modes. Then stochastic eigensolutions of Eq. (22) are expressed as follows

$$\begin{aligned}\widetilde{\mu}_i&=\left(\overline{\mu}_i+\sigma_{\mu_i}\varepsilon\right)\\ \widetilde{\phi}_i&=\left(\overline{\phi}_i+\sigma_{\phi_i}\varepsilon\right)\end{aligned} \quad (23)$$

Using polynomial chaos projection of variables in the Eq. (22), extract their mean value $\overline{(.)}$ and standard deviation $(\sigma)$. The explicit expression for the standard deviation of eigenvalues and eigenvectors obtained from the stochastic quadratic eigenvalue problem are given below. A detailed derivation is given in Appendix C.

The explicit expression for the standard derivation of the eigenvalues ($\sigma_{\mu_i}$) is

$$\begin{aligned}
\sigma_{\mu_i} = &\left(\overline{\Phi}_q\right)_i^T \Big[(\sigma_{D_{21}}^T + \sigma_{D_{43}}^T + (\sigma_{D_{41}}\lambda_y^{-1})^T + (\sigma_{D_{23}}\lambda_y)^T) + \overline{\mu}_i I_{2n}(\sigma_{D_{11}}^T + \sigma_{D_{22}}^T + \sigma_{D_{33}}^T + \sigma_{D_{44}}^T + (\sigma_{D_{31}}\lambda_y^{-1})^T + (\sigma_{D_{42}}\lambda_y^{-1})^T \\
&+(\sigma_{D_{13}}\lambda_y)^T + (\sigma_{D_{24}}\lambda_y)^T) + \overline{\mu}_i^2 I_{2n}(\sigma_{D_{12}}^T + \sigma_{D_{34}}^T + (\sigma_{D_{32}}\lambda_y^{-1})^T + (\sigma_{D_{14}}\lambda_y)^T)\Big] \Big[(\overline{D}_{21}^T + \overline{D}_{43}^T + (\overline{D}_{41}\lambda_y^{-1})^T + (\overline{D}_{23}\lambda_y)^T) \\
&+ \sigma_{\mu_i} I_{2n}(\overline{D}_{11}^T + \overline{D}_{22}^T + \overline{D}_{33}^T + \overline{D}_{44}^T + ((\overline{D}_{31} + \overline{D}_{42})\lambda_y^{-1})^T + ((\overline{D}_{13} + \overline{D}_{24})\lambda_y)^T) + \overline{\mu}_i^2 I_{2n}(\overline{D}_{12}^T + \overline{D}_{34}^T + (\overline{D}_{32}\lambda_y^{-1})^T + (\overline{D}_{14}\lambda_y)^T\Big]^{-1} \\
&+ \Big[(\overline{D}_{21} + \overline{D}_{43} + (\overline{D}_{41}\lambda_y^{-1})(\overline{D}_{23}\lambda_y)) + \overline{\mu}_i^{-1} I_{2n}(\overline{D}_{11} + \overline{D}_{22} + \overline{D}_{33} + \overline{D}_{44} + (\overline{D}_{31} + \overline{D}_{42})\lambda_y^{-1} + (\overline{D}_{13} + \overline{D}_{24})\lambda_y) \\
&+\overline{\mu}_i^{-2} I_{2n}(\overline{D}_{12} + \overline{D}_{34} + \overline{D}_{32}\lambda_y^{-1} + \overline{D}_{14}\lambda_y)\Big] - \left(\overline{\Phi}_q\right)_i^T \Big[(\sigma_{D_{21}} + \sigma_{D_{43}} + \sigma_{D_{41}}\lambda_y^{-1} + \sigma_{D_{23}}\lambda_y) + \overline{\mu}_i^{-1} I_{2n}(\sigma_{D_{11}} + \sigma_{D_{22}} + \sigma_{D_{33}} \\
&+\sigma_{D_{44}} + \sigma_{D_{31}}\lambda_y^{-1} + \sigma_{D_{42}}\lambda_y^{-1} + \sigma_{D_{13}}\lambda_y + \sigma_{D_{24}}\lambda_y) + \overline{\mu}_i^{-2} I_{2n}\left(\sigma_{D_{12}} + \sigma_{D_{34}} + \sigma_{D_{32}}\lambda_y^{-1} + \sigma_{D_{14}}\lambda_y\right)\Big] \\
&\Big[\left(\overline{\Phi}_q\right)_i^T \Big[-(\overline{D}_{11}^T + \overline{D}_{22}^T + \overline{D}_{33}^T + \overline{D}_{44}^T + (\overline{D}_{31}\lambda_y^{-1})^T + (\overline{D}_{42}\lambda_y^{-1})^T) - 2\overline{\mu}_i I_{2n}(\overline{D}_{12}^T + \overline{D}_{34}^T + (\overline{D}_{32}\lambda_y^{-1})^T + (\overline{D}_{14}\lambda_y)^T)\Big] \\
&\Big[(\overline{D}_{21}^T + \overline{D}_{43}^T + (\overline{D}_{41}\lambda_y^{-1})^T + (\overline{D}_{23}\lambda_y)^T) + \overline{\mu}_i I_{2n}(\overline{D}_{11}^T + \overline{D}_{22}^T + \overline{D}_{33}^T + \overline{D}_{44}^T + ((\overline{D}_{31} + \overline{D}_{42})\lambda_y^{-1})^T + (\overline{D}_{13} + \overline{D}_{24})\lambda_y^T) \\
&+\overline{\mu}_i^2 I_{2n}(\overline{D}_{12}^T + \overline{D}_{34}^T + (\overline{D}_{32}\lambda_y^{-1})^T + (\overline{D}_{14}\lambda_y))^T\Big]^{-1} \Big[(\overline{D}_{21} + \overline{D}_{43} + (\overline{D}_{41}\lambda_y^{-1}) + (\overline{D}_{23}\lambda_y)) + \overline{\mu}_i^{-1} I_{2n}(\overline{D}_{11} + \overline{D}_{22} + \overline{D}_{33} \\
&+\overline{D}_{44} + (\overline{D}_{31} + \overline{D}_{42})\lambda_y^{-1} + (\overline{D}_{13} + \overline{D}_{24})\lambda_y) + \overline{\mu}_i^{-2} I_{2n}(\overline{D}_{12} + \overline{D}_{34} + \overline{D}_{32}\lambda_y^{-1} + \overline{D}_{14}\lambda_y)\Big] - \left(\overline{\Phi}_q\right)_i^T \\
&\Big[\overline{\mu}_i^{-2} I_{2n}(\overline{D}_{11} + \overline{D}_{22} + \overline{D}_{33} + \overline{D}_{44} + (\overline{D}_{31} + \overline{D}_{42})\lambda_y^{-1} + (\overline{D}_{13} + \overline{D}_{24})\lambda_y) + 2\overline{\mu}_i^{-3} I_{2n}(\overline{D}_{12} + \overline{D}_{34} + \overline{D}_{32}\lambda_y^{-1} + \overline{D}_{14}\lambda_y)\Big]\Big]^{-1}
\end{aligned} \tag{24}$$

Analogously, the explicit expression for the standard deviation of the eigvenvectors ($\sigma_{(\Phi_q)_i}$) is

$$\begin{aligned}
\sigma_{(\Phi_q)_i} = -\Big[&(\sigma_{D_{21}} + \sigma_{D_{43}} + \sigma_{D_{41}}\lambda_y^{-1} + \sigma_{D_{23}}\lambda_y) + \sigma_{\mu_i} I_{2n}(\overline{D}_{11} + \overline{D}_{22} + \overline{D}_{33} + \overline{D}_{44} + (\overline{D}_{31} + \overline{D}_{42})\lambda_y^{-1} \\
&+(\overline{D}_{13} + \overline{D}_{24})\lambda_y) + \overline{\mu}_i I_{2n}(\sigma_{D_{11}} + \sigma_{D_{22}} + \sigma_{D_{33}} + \sigma_{D_{44}} + \sigma_{D_{31}}\lambda_y^{-1} + \sigma_{D_{42}}\lambda_y^{-1} + \sigma_{D_{13}}\lambda_y + \sigma_{D_{24}}\lambda_y) \\
&+2\overline{\mu}_i I_{2n}\sigma_{\mu_i}(\overline{D}_{12} + \overline{D}_{34} + \overline{D}_{32}\lambda_y^{-1} + \overline{D}_{14}\lambda_y) + \overline{\mu}_i^2 I_{2n}(\sigma_{D_{12}} + \sigma_{D_{34}} + \sigma_{D_{32}}\lambda_y^{-1} + \sigma_{D_{14}}\lambda_y)\Big]\left(\overline{\Phi}_q\right)_i \\
&\Big[(\overline{D}_{21} + \overline{D}_{43} + \overline{D}_{41}\lambda_y^{-1} + \overline{D}_{23}\lambda_y) + \overline{\mu}_i I_{2n}(\overline{D}_{11} + \overline{D}_{22} + \overline{D}_{33} + \overline{D}_{44} + (\overline{D}_{31} + \overline{D}_{42})\lambda_y^{-1} + (\overline{D}_{13} + \overline{D}_{24})\lambda_y) \\
&+ \overline{\mu}_i^2 I_{2n}(\overline{D}_{12} + \overline{D}_{34} + \overline{D}_{32}\lambda_y^{-1} + \overline{D}_{14}\lambda_y)\Big]^{-1}
\end{aligned} \tag{25}$$

Above Eq. (24) and Eq. (25) are the explicit expressions for the statistics of wave propagation using deterministic eigenvalue solutions in the periodic media for the 2D cases.

### *3.2. Internal nodes*

If the modeling of cells need inner DOFs, a condensed dynamic stiffness matrix is necessary. In case of internal node ($I$) (Fig. 5), the DOFs are partitioned into the boundary DOFs ($D_{bd}$) and internal DOFs ($D_I$). The dynamic stiffness matrix has the following form

$$D = \begin{bmatrix} \widehat{D}_{bdbd} & \widehat{D}_{bdI} \\ \widehat{D}_{Ibd} & \widehat{D}_{II} \end{bmatrix} \tag{26}$$

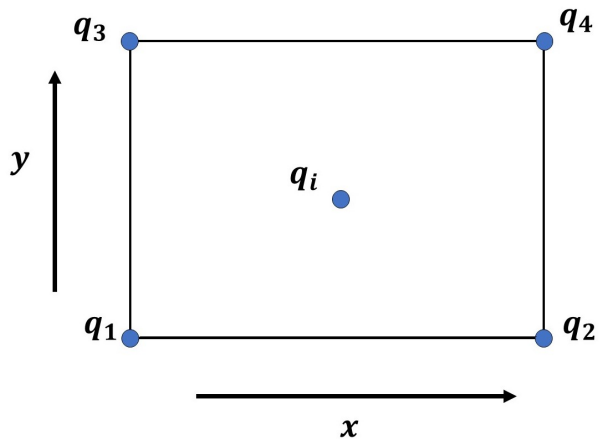


Figure 5: Schematic diagram of a thin plate element with inner nodes

where symbol $\widehat{(.)}$ represents the elements from the original dynamic stiffness matrix. The standard deviation of the condensed dynamic stiffness matrix (derived in Appendix B) can be expressed as

$$\sigma_{D_{bd}} = \left[\sigma_{\widehat{D}_{bdbd}}\right] - \left[\overline{\overline{\widehat{D}}}_{bdI} \quad \sigma_{\widehat{D}_{bdI}}\right] \begin{bmatrix} \overline{\overline{\widehat{D}}}_{II}^{-1} & -\overline{\overline{\widehat{D}}}_{II}^{-1} \sigma_{\widehat{D}_{II}} \overline{\overline{\widehat{D}}}_{II}^{-1} \\ 0 & \overline{\overline{\widehat{D}}}_{II}^{-1} \end{bmatrix} \begin{bmatrix} \sigma_{\widehat{D}_{Ibd}} \\ \overline{\overline{\widehat{D}}}_{Ibd} \end{bmatrix} \tag{27}$$

where symbol $\overline{\overline{\widehat{(.)}}}$ represent the mean value from the original dynamic stiffness matrix.

## 4. Numerical results and discussion

The proposed numerical scheme is summarized in the workflow in Fig. 6. In this section, the validation of the developed stochastic WFEM based on quadratic eigenvalue (SWFEM QEV) formulation is carried out. In the first part, the validation of SWFEM QEV for the 1D periodic rod with band gap is presented. Also, the validation of the metamaterial case is discussed. In the second part, the SWFEM QEV formulation is validated for the homogeneous and periodic plate and the applicability and accuracy of the formulation is checked.

### *4.1. Validation of SWFEM QEV: 1D (longitudinal waves)*

This subsection includes the validation of the SWFEM QEV formulation applied to a 1D periodic rod considering the material uncertainty; also the variation of the wavenumber is analyzed with the variation of the input properties.

#### *4.1.1. Dispersion analysis of periodic rod*

Periodic rod consists of section A of length $l_1$ and section B of length $l_2$ as depicted in the Fig.7. Here cells A and B are made of different materials. The validation of the present developed formulation is demonstrated by comparing the result with those available from analytical sampling and MCS. The SWFEM QEV is used to study the effect of

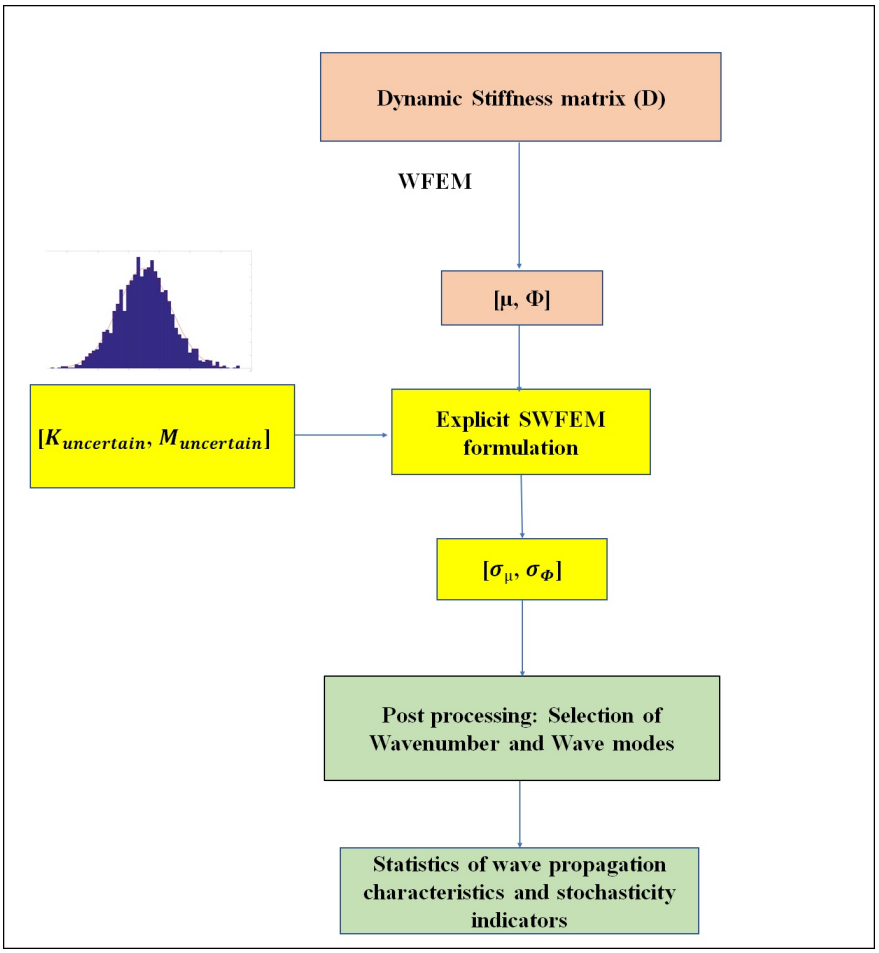


Figure 6: Workflow of developed SWFEM

parametric uncertainties on the dispersion relation of the longitudinal wave in periodic rod with sections A and B made of epoxy and aluminium respectively. The length of $l_1$ and $l_2$ are 1m each with a circular cross section of a radius of 0.0644m.

The reference analytical solution of a periodic rod is based on the following expression of the wavenumber [38]

$$\cos(kl) = \cos\left(\frac{\omega}{c_a} l_a\right) \cos\left(\frac{\omega}{c_b} l_b\right) - \frac{1}{2}\left(\frac{\rho_a c_a}{\rho_b c_b} + \frac{\rho_b c_b}{\rho_a c_a}\right) \sin\left(\frac{\omega}{c_a} l_a\right) \sin\left(\frac{\omega}{c_b} l_b\right) \tag{28}$$

where $c_a$, $c_b$ is the wave velocity in the section A and B respectively and expressed as $c_a = \sqrt{E_a/\rho_a}$ and $c_b = \sqrt{E_b/\rho_b}$, $E_a$, $\rho_a$, $l_a$ are the Young's modulus, the density and length for section A and $E_a$, $\rho_a$, $l_b$ for the section B. $l$ is the total length of the unit cell.

Here the stochastic wave finite element method based on transfer matrix (SWFEM TM) [16] is extended to 1D periodic media by finding the standard deviation of the condensed dynamic stiffness matrix. A detailed reminder of SWFEM TM is presented in Appendix E.

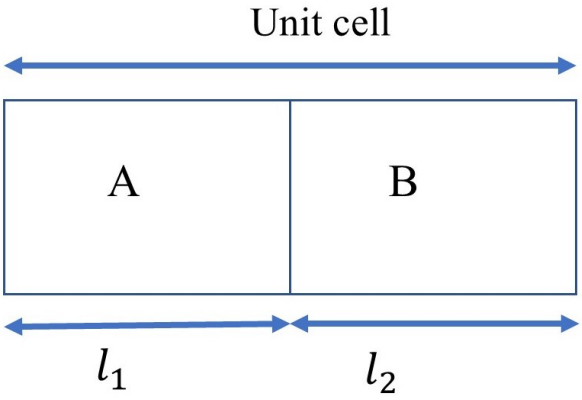


Figure 7: Symmetric unit cell of 1D periodic rod

The uncertainty effect is studied considering a variation of (4%) of the Young's modulus nominal values. It is to be mentioned that the input uncertainties are represented inside the bracket (x). The frequency range is up to 2000 Hz. The sampling method with 10000 samples is used to get the wave characteristics of the analytical wavenumber obtained using Eq. (28). As number of number of samples is increased the sampling error is decreased so 10000 samples are chosen to obtain the reference results. The analytical sampling and MCS results are treated as reference result for validation purpose.

Two node rod element is considered. This element allows treatments of longitudinal wave. The local stiffness and mass matrices are assembled into global stiffness and mass matrices in the MATLAB environment with 200 elements in the unit cell of the periodic rod. In this way, the wavelength contains at least 20 elements in the frequency range. The material and geometric properties are reported in Table 1.

Table 1: Material and geometric properties of periodic rod

| Geometry/Property | Value |
|---|---|
| Rod length (A) | 1 $m$ |
| Rod length (B) | 1 $m$ |
| Radius of rod | 0.0644 $m$ |
| Young's modulus (A) | $4.50 \times 10^9$ $Pa$ |
| Young's modulus (B) | $70 \times 10^9$ $Pa$ |
| Mass density (A) | 1200 $kg/m^3$ |
| Mass density (B) | 2700 $kg/m^3$ |
| Loss factor (A) and (B) | 0.001 |

The results obtained with analytical sampling, SWFEM TM, SWFEM QEV, and wave finite method Monte Carlo

simulation (WFEM MCS) are compared. The mean values comparison is shown in Fig. 8; there exist two full band gaps, first at approximately 418-928 Hz and the other 1184-1847 Hz. It is to be noted that the WFEM MCS are performed on WFEM quadratic form. The comparison of the standard deviation is presented in Fig. 9. The results are in good agreement. The SWFEM QEV standard deviation is computed considering loss factor on the contrary the analytical sampling is computed without damping. It is observed that the effect of the uncertainty on the longitudinal wavenumber, at the start of the first band gap, is nearly 3% and 10% nearly at the end of the band gap. With increasing frequency, the uncertainty effect is growing as seen that variation is around 33% at the start of second bandgap frequency and 35% at the end of the second band gap frequency. It suggests that the effect of the uncertainty is increasing with increasing frequency range for longitudinal wavenumber, as expected.

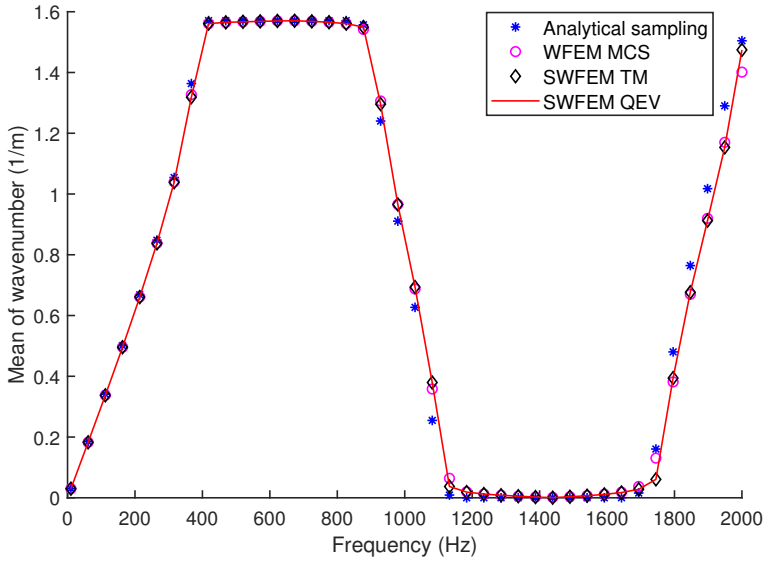


Figure 8: Mean value of longitudinal wavenumber comparison (Young's modulus stochastic)

### *4.1.2. Effect of the uncertain parameter on the wavenumber in the periodic rod*

The variation of material parameter scatters the longitudinal wavenumber. Here the focus is to quantify the variation of the coefficient of variation (COV) which is defined as (standard deviation /mean value) for the longitudinal wavenumber with the variation of COV of the material properties; it also helps to judge the capacity of the developed formulation for the range of variation it can accommodate. In the numerical experiment, the material properties, namely Young's modulus and density, are varying with Gaussian distribution. For the comparison 10000 samples are used for the WFEM MCS. The input in term of COV is varying up to (7%) about the mean value of the considered parameter. In the first case, Young's modulus is stochastic. The comparison of the COV of the input parameter (Young's modulus stochastic) at discrete frequencies are shown in Fig. 10. From the figure, it is observed that in the

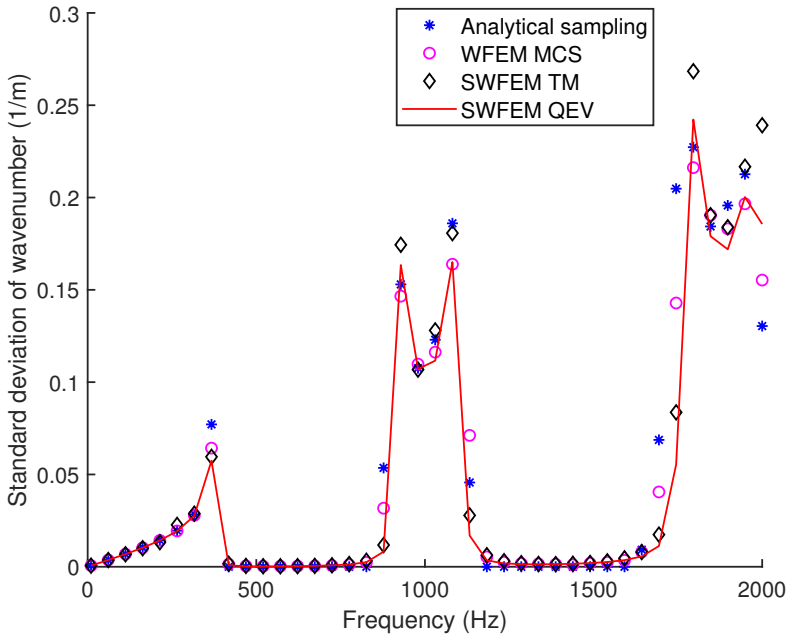


Figure 9: Standard deviation of longitudinal wavenumber comparison (Young's modulus stochastic)

propagation frequency region, the variation the wavenumber is linear; however, this is not withheld when it comes to the edge of the band gap frequency. In the low frequency, the variation of wavenumber is significantly affected by the variation of the input uncertainty. The highest variation is recorded at the second band gap edge frequency.

The comparison of stochastic density is shown in Fig. 11. The same behaviour is visible in case of the stochastic density. From the graph, it is confirmed that the validity of the developed formulation is limited to roughly 4% variation. It is because of the fact that the formulation is based on the first order expansion. The effect of elasticity stochasticity is higher than the stochastic density. Also, the significance of the uncertain wavenumber is increasing with the increasing frequency of the interest.

### *4.1.3. Dispersion analysis of metamaterial rods*

To demonstrate the capability of the developed stochastic formulation to work with a metamaterial system; a simple metamaterial based rod system is considered. The system consisting of a uniform rod with a periodically attached single degree of freedom (SDOF) local resonators, is evaluated. The metamaterial rod system material and geometrical parameters are as presented in Table 2.

The local resonator frequency of the SDOF resonator is tuned to 500 Hz with a mass ratio of 20% of the host system. The resonator with the stiffness $1.6743\times10^{6}N/m$ and mass of 0.1696 kg is attached to the left end of the host rod. The uncertainty in the host rod is considered in Young's modulus with (4%) around the nominal value. The comparison for WFEM MCS, SWFEM QEV and SWFEM TM is presented. The mean value comparison is shown

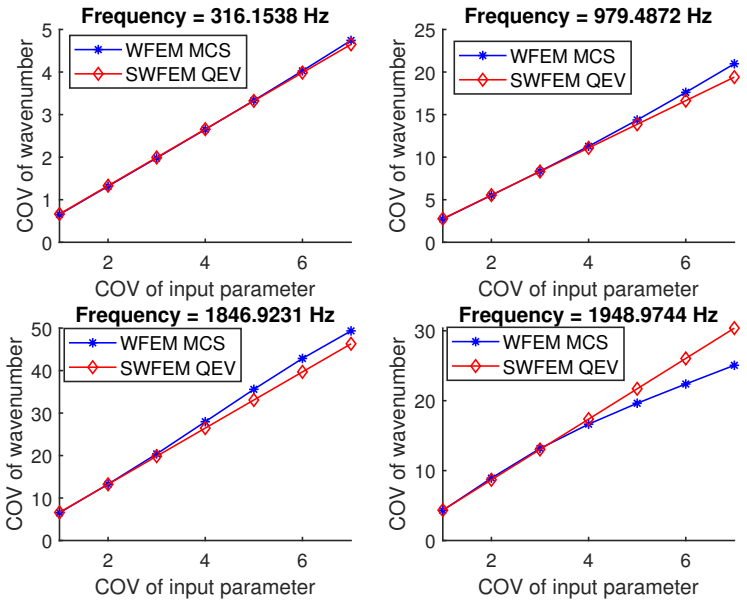


Figure 10: Variation of the longitudinal wavenumber with varying Young's modulus, MCS with 10000 samples (blue star line) and present formulation (red diamond line) at discrete frequency

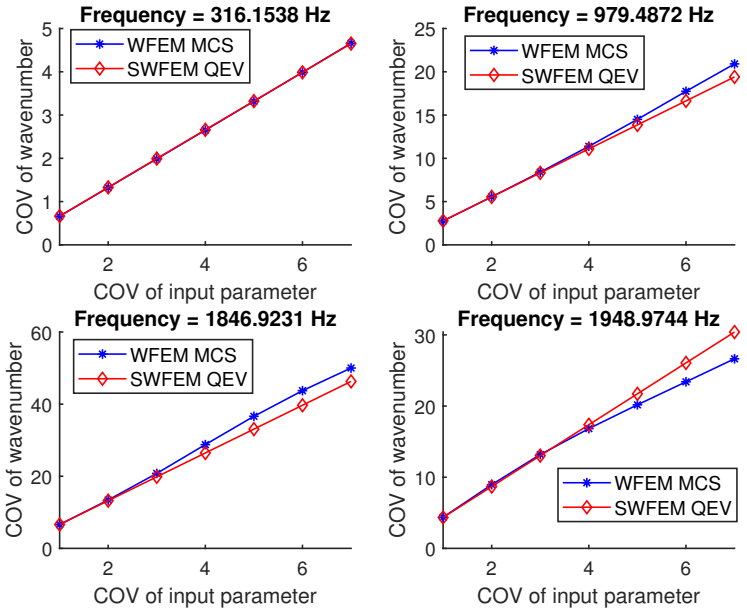


Figure 11: Variation of the longitudinal wavenumber with varying density, MCS with 10000 samples (blue star line) and present formulation (red diamond line) at discrete frequency

Table 2: Metamaterial rod material and geometric properties

| Geometry/Property | Value |
|---|---|
| Rod length | 1 $m$ |
| Radius of rod | 0.01 $m$ |
| Young's modulus | $70 \times 10^9$ $Pa$ |
| Mass density | $2700 \times 10^9$ $Pa$ |
| Loss factor | 0.01 |

in Fig. 12 and standard deviations comparison in Fig. 13. It can seen from the graphs, the curves are in excellent agreement which confirms the validity of the formulation for the simulation of uncertainty in the metamaterial system. In Fig. 12 a typical asymmetric resonance gap observed with sharp attenuation at resonator tuned frequency (500 Hz) of the SDOF resonator. In the lower tuned frequency, the nature of such attenuation is asymmetric. An indicator is used to check the effects of uncertainties. Stochasticity indicator is defined as the ratio of the standard deviation of the wavenumber and the mean of the wavenumber at a discrete frequency. It is also expressed as coefficient of variation (COV):

$$COV = \sigma_k / \overline{k} \tag{29}$$

where $\sigma_k$ is the standard deviation of the wavenumber and $\overline{k}$ is the mean value of wavenumber. It indicates the spread of the wavenumber at discrete frequency step. The stochastic indicator for the metamaterial system is presented in Fig. 14. From the graph it is visible that roughly 2% variation of the propagative longitudinal wavenumber exist. When it comes about the resonance band gap, the variation of 2.63% of the wavenumber occurs at the start of resonance band gap frequency (492 Hz) and maximum variation of 2.7% of the wavenumber at the end of resonance band gap frequency (552 Hz). Inside the resonance band gap, the variation of wavenumber attains it minimum with 1.4% variation. However; it is not completely zero. As a matter of fact, the results shows that the uncertainty alters the wave states inside the resonance band gap and uncertainties effects are increasing in higher frequency. Also, the results obtained from the SWFEM QEV are in excellent agreement with the WFEM MCS results inside the resonance band gap.

#### *4.1.4. Effect of the uncertain parameter on the wavenumber of metamaterial rod*

To assess the effect of the uncertain input to the variation of the wavenumber of the metamaterial rod system, the uncertainty in the host structure is considered. The variation of the wavenumber on the variation of Young's modulus is plotted in Fig. 15. In the case of stochastic density, the variations are shown in Fig. 16. From the graphs, it can be observed that with stochastic elastic modulus, the effect on wavenumber is showing linear trends. However; with uncertainty density, the band gap widens slightly. Also, around the resonance frequency, effect of the uncertainty is nearly minimum. It is noteworthy that in the case of the metamaterial and stochastic host structure, the quadratic

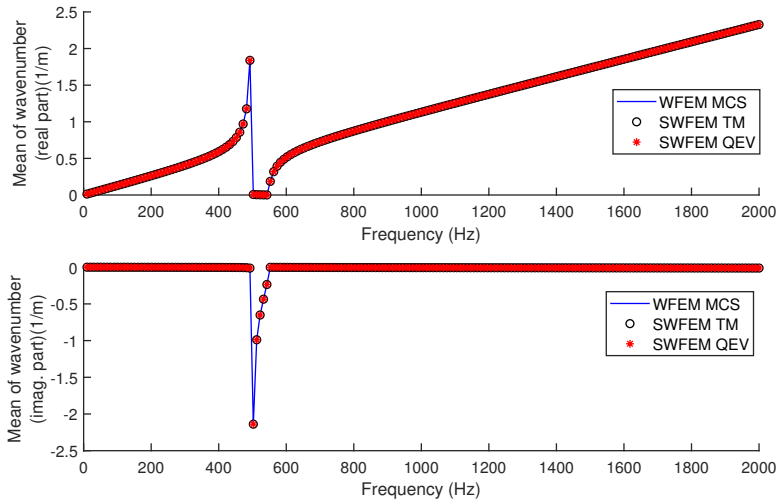


Figure 12: Mean value of the real and imaginary part of longitudinal wavenumber comparison (Young's modulus stochastic)

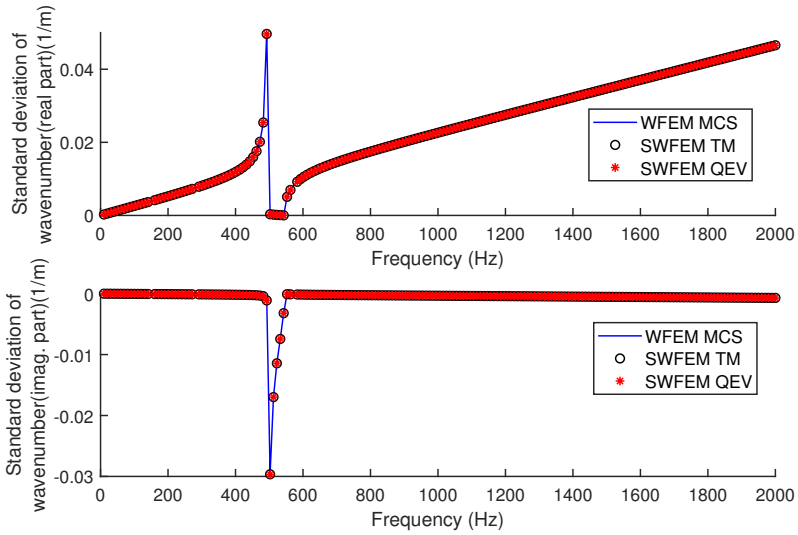


Figure 13: Standard deviation of the real and imaginary part of longitudinal wavenumber comparison (Young's modulus stochastic)

formulation can handle a higher level of uncertainties.

### *4.2. Validation of SWEFM QEV: 2D (flexural waves)*

In this section, numerical studies are presented to demonstrate the validity and applicability of the stochastic quadratic formulation developed in the paper. Two cases, namely homogenous plate case and periodic plate case are discussed; also the wavenumber dispersion is analyzed with the variation of the input parameters.

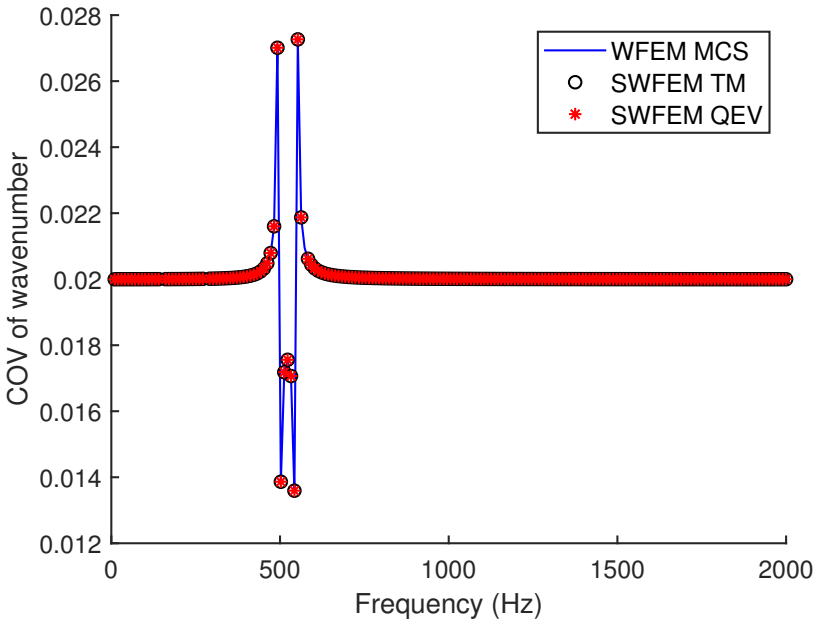


Figure 14: Stochasticity indicator for metamaterial rod system (Young's modulus stochastic)

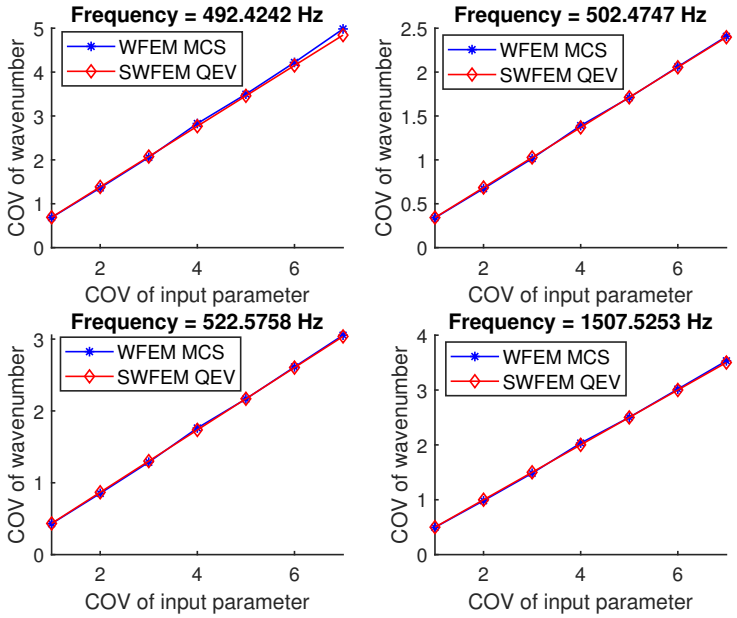


Figure 15: Variation of the longitudinal wavenumber with host structure uncertainty (Young's modulus stochastic), MCS with 10000 samples (blue star line) and present formulation (red diamond line) at discrete frequency

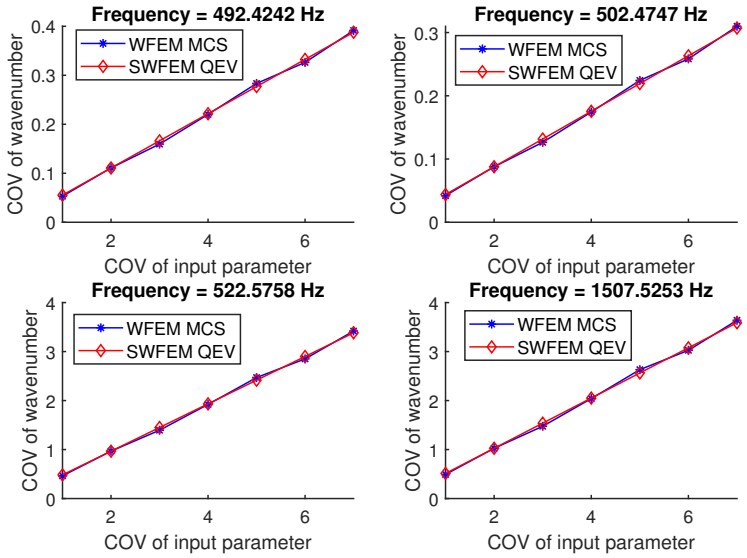


Figure 16: Variation of the longitudinal wavenumber with host structure uncertainty (density stochastic), MCS with 10000 samples (blue star line) and present formulation (red diamond line) at discrete frequency

### *4.2.1. Homogeneous plate*

To demonstrate the validity of the formulation in the simple homogenous plate case, numerical simulations are performed. A thin plate unit cell is modelled with four node elements with three DOFs at each node. The material and geometrical properties are reported in Table 3. The sides of the unit cell are $L_x = L_y = 0.005m$ with thickness

Table 3: Material properties for homogeneous plate

| Geometry/Property | Value |
|---|---|
| Young's modulus | $210 \times 10^9\ Pa$ |
| Poission's ratio | 0.3 |
| Mass density | $7800\ kg/m^3$ |
| Loss factor | 0.01 |

$h = 0.0005m$. The reference analytical solution of a plate is based on following expression of the wavenumber

$$k_f = \sqrt[4]{\rho h \omega^2 / D_{bending}} \tag{30}$$

where plate bending stiffness is $D_{\text{bending}} = Eh^3/12\left(1-\nu^2\right)$. $E$ is the Young's modulus, $\rho$ is the density, $\nu$ is the Poission's ratio, $h$ is the plate thickness and $\omega$ is the circular frequency. The uncertainty effect is studied with variation of (4%) of the Young's modulus around nominal value. The out of plane flexural wave is responsible for transmitting most of the acoustic energy. Therefore out of plane flexural wave is the primary wave type taken into account during

the numerical analysis. The analytical sampling and WFEM MCS results (both with 10000 samples) are treated as reference results for the validation purpose. The mean value comparison of the flexural wavenumber is presented in Fig. 17. Also the standard deviation comparison is shown in Fig. 18. The standard deviation is obtained from the SWFEM QEV is in excellent agreement with analytical sampling and WFEM MCS resutls. This verifies the validity of the stochastic quadratic formulation for the homogenous plate. The stochasticity indicator for the (4%) variation in the Young's modulus is plotted and shown in Fig. 19. From the figure it can be inferred that Young's modulus uncertainty does not shows any variation on the out of plane flexural wavenumber with the frequency. The dispersion curve in the $(k_x, k_y)$ plane at discrete frequencies are presented in Fig. 20. The mean and standard deviation comparison is shown in the Fig. 20 for the discrete frequencies. From Fig. 20 it can be observed that the contours curves are independent of propagation direction. This is in fact due to the isotropic nature of the plate. There the material properties are independent of the direction and, this is also predicted in the simulated results.

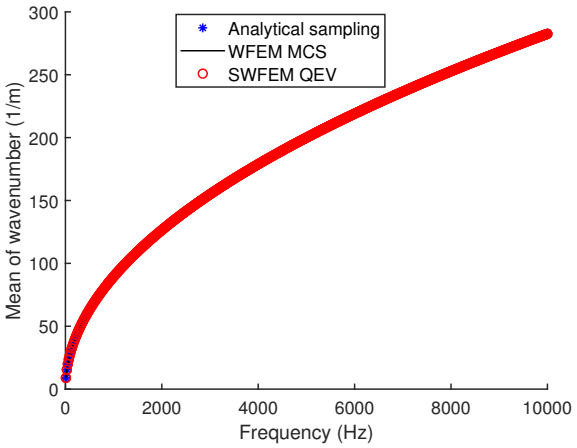


Figure 17: Mean value of out of plane flexural wavenumber in $x$ direction (Young's modulus stochastic)

### *4.2.2. Effect of the uncertain parameter on out of plane flexural wavenumber of homogeneous plate*

The influence of the uncertainties in the material property on the variation of out of plane flexural wavenumber is discussed. The COV of the wavenumber with change of input COV for the range from (1%) to (7%) is analyzed. In first case, only Young's modulus considered as an uncertain input. The comparison of the COV of the flexural wavenumber obtained from SWFEM QEV and COV of the WFEM MCS results are presented in Fig. 21. From Fig. 21 it can be seen that the flexural wavenumber variation is linear. In the second case, the density is considered as the uncertain input parameter. The comparison is presented in Fig. 22; and linear variation of the wavenumber is observed. In both cases, the results obtained from SWFEM QEV is very close with the reference WFEM MCS results. It shows the accuracy of the formulation for the range of COV considered. From Fig. 21 and Fig. 22, it can also be seen that the variations of the flexural wavenumber is slightly higher with uncertain Young's modulus than the

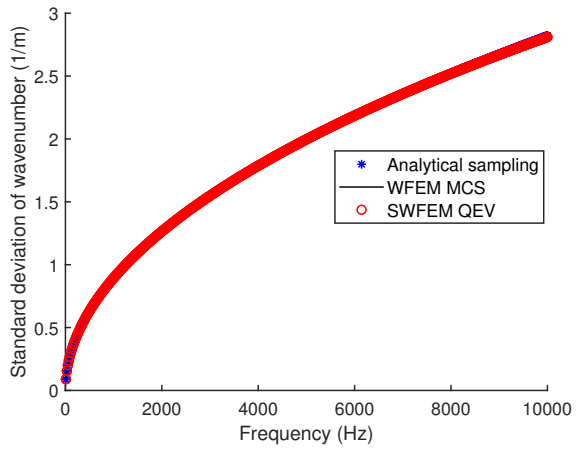


Figure 18: Standard deviation out of plane flexural wavenumber in $x$ direction (Young's modulus stochastic)

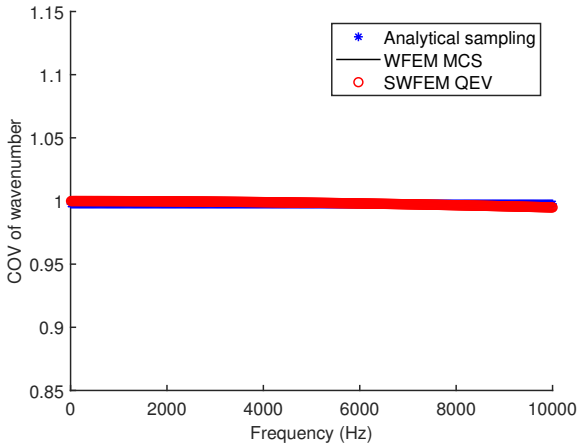


Figure 19: Stochasticity indicator for out of plane flexural wavenumber in $x$ direction (Young's modulus stochastic)

uncertain density.

### *4.2.3. Periodic plate*

In this subsection, validation of the SWFEM QEV formulation is performed for 2D perioidic plate. Also the flexural wavenumber dispersion statistics is analyzed with variation of the input parameters. The periodic plate contains N repeating unit cell in both $x$ and $y$ direction. Each unit cell consists of an assembly of a 2x2 array of unit cells made with sub-plate type A and sub-plate type B. The material properties of the sub-plate types A and B are different. The schematic of periodic plate and corresponding unit cell model is shown in Fig. 23. The considered material properties are reported in Table 4. The periodic plate unit cell is modeled with four noded elements with three DOFs at each node. The sides of the unit cell are $L_x = L_y = 0.1m$ with thickness $h = 0.01m$.

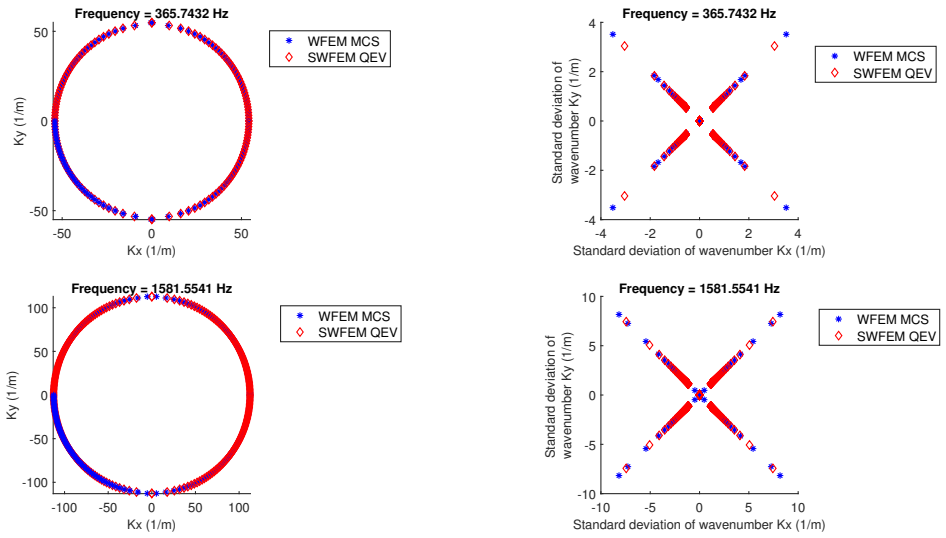


Figure 20: k-space mean value and standard deviation (Young's modulus stochastic), MCS results (blue star) and present formulation (red diamond) at discrete frequency

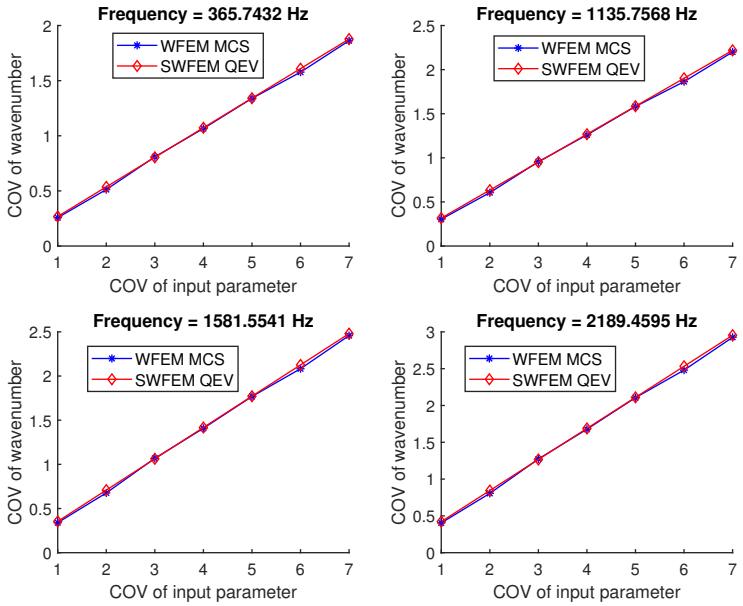


Figure 21: Variation of the out of plane flexural wavenumber (Young's modulus stochastic), MCS with 10000 samples (blue star line) and present formulation (red diamond line) at discrete frequency

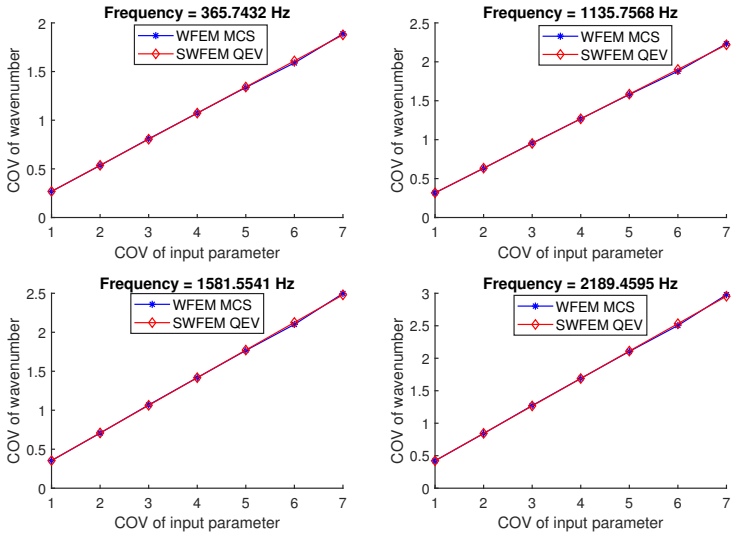


Figure 22: Variation of the out of plane flexural wavenumber (density stochastic), MCS with 10000 samples (blue star line) and present formulation (red diamond line) at discrete frequency

Table 4: Material properties for homogeneous plate

| Geometry/Property | Value |
|---|---|
| Young's modulus of sub-plate type A | $70 \times 10^9$ $Pa$ |
| Young's modulus of sub-plate type B | $4.5 \times 10^9$ $Pa$ |
| Poission's ratio of sub-plate type A and B | 0.3 |
| Mass density of sub-plate type A | 2700 $kg/m^3$ |
| Mass density of sub-plate type B | 1200 $kg/m^3$ |
| Loss factor of sub-plate type A and B | 0.01 |

The validation of the developed formulation is presented for out of plane flexural wavenumber. The considered frequency range is upto 3000 Hz. The Young's modulus of sub-plate type A and sub-plate type B are considered uncertain. The variation of (4%) about the nominal values of Young's modulus is studied. Since there is no results reported in the literature for the the periodic plate with uncertainties, the WFEM MCS with 10000 samples is considered as the reference solution. Using $(\omega, k_y)$ formulation the flexurual wavenumber dispersion is computed and comparison of the mean value and standard derivation is shown in Fig. 24 and Fig. 25 respectively. The comparison shows the agreement of the SWFEM QEV results with the reference results. It verifies the applicability of formulation for periodic plate case. From the mean value comparison shown in Fig. 24, it can be observed, the start of the band gap is approximately at 2352 Hz. At the same frequency maximum value of standard deviation is observed in the

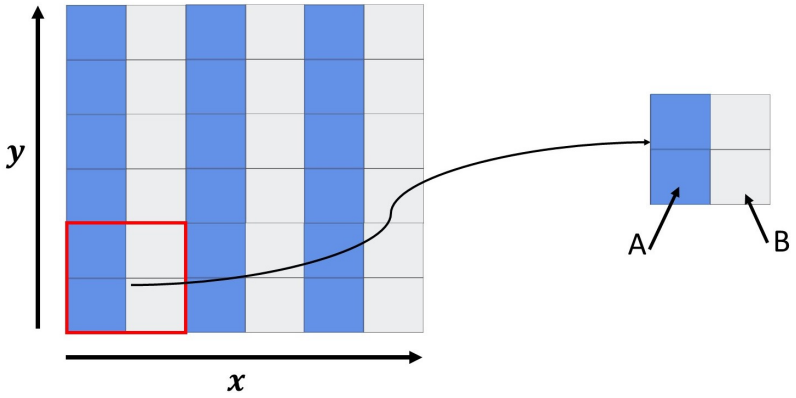


Figure 23: Schematic of the periodic plate and unit cell of the periodic plate

standard deviation comparison graph shown in Fig. 25. Also inferring to the stochasticity indicator presented in Fig. 26, the maximum variation of 6.5% of the wavenumber is observed at 2352 Hz. Inside the band gap zone, the variation of wavenumber shows the decrease in value of the standard deviation.

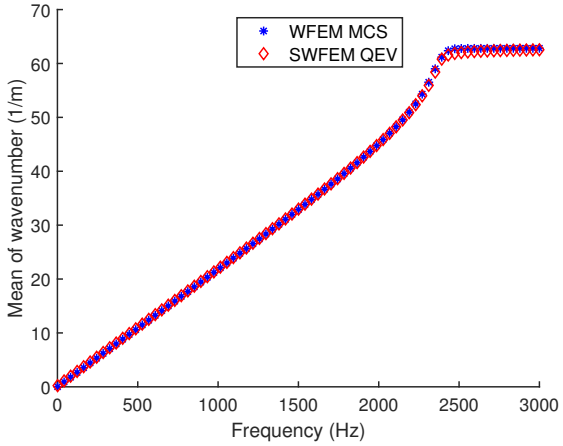


Figure 24: Mean value of out of plane flexural wavenumber in $x$ direction (Young's modulus stochastic)

The dispersion curve in the $(k_x, k_y)$ plane at discrete frequencies are shown in Fig.27. From Fig.27, It can be seen that the contour curves are dependent on the propagation direction. It is due to the periodicity of the plate. It can be summaries that the uncertainties affects the out of plane flexural wavenumber scattering and maximum value of the variation of out of plane flexural wavenumber occurs at the band gap edge frequencies.

*4.2.4. Effect of the uncertain parameter on the out of plane flexural wavenumber of periodic plate*

The COV of the out of plane flexural wavenumber with uncertain Young's modulus and uncertain density are analyzed. The scattering of the out of plane flexural wavenumber can be taken by allowing the COV of the material

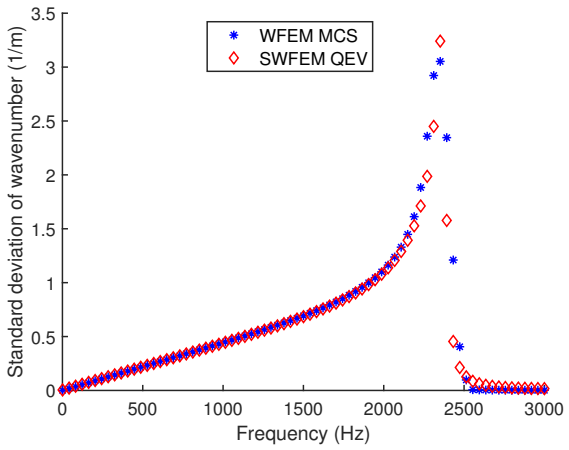


Figure 25: Standard deviation out of plane flexural wavenumber in $x$ direction (Young's modulus stochastic)

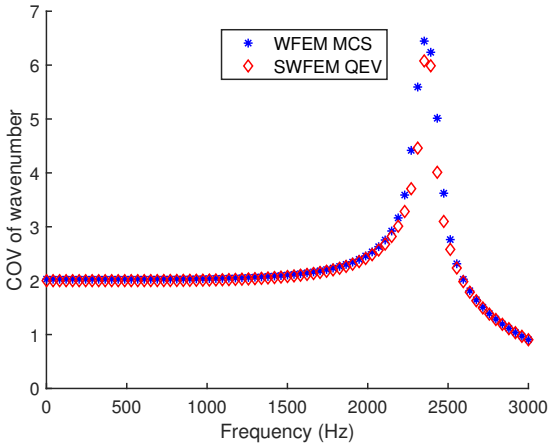


Figure 26: Stochasticity indicator for out of plane flexural wavenumber in $x$ direction (Young's modulus stochastic)

parameters to vary in the range from (1%) to (7%). In this range, the presented results would be enough to extrapolate the results for the COV keeping in mind the limitation of the first-order perturbation method. The variation of the out of plane flexural wavenumber for the periodic plate with uncertainty in Young's modulus is shown in Fig. 28, and with uncertainty in density is shown in Fig. 29. It can be observed that the flexural wavenumber COV for the uncertain elasticity is higher than uncertain density. This difference in COV is very minimal and can be seen mostly with increasing frequency. The COV plots shown the linear variation of out of plane flexural wavenumber in low frequency regions, and shifting to higher variation with increasing frequency.

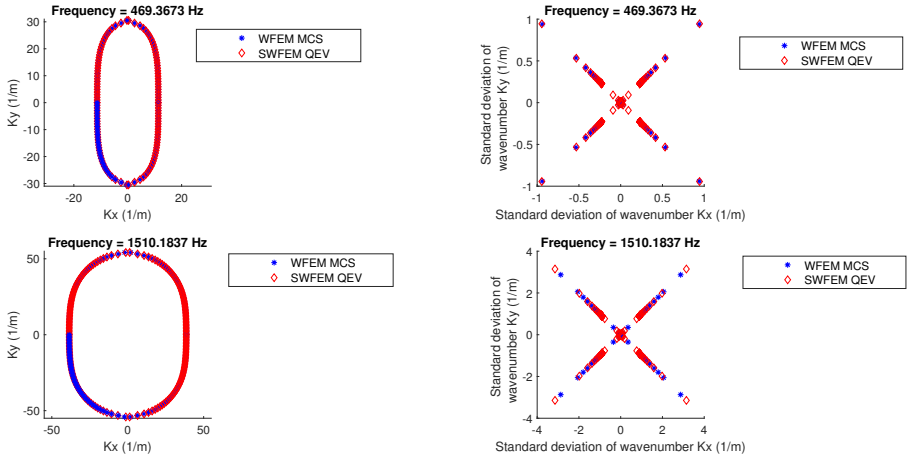


Figure 27: k-space mean value and standard deviation of wavenumber (Young's modulus stochastic)

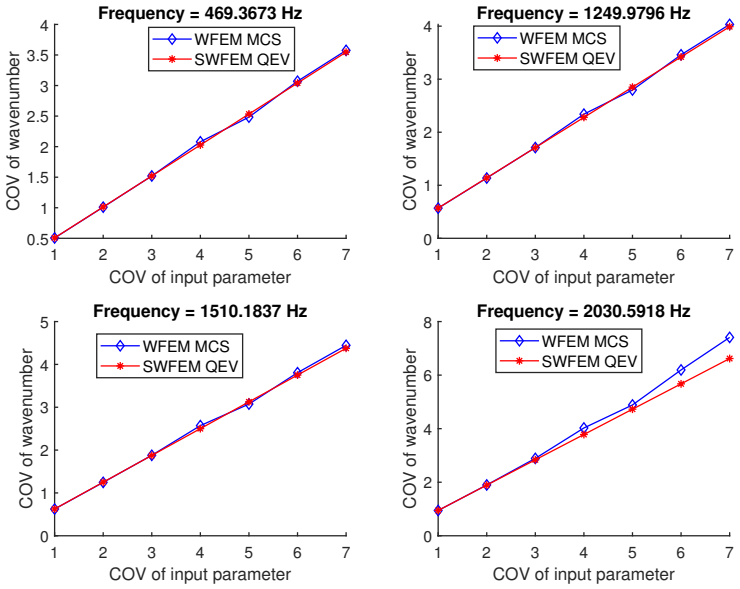


Figure 28: Variation of the out of plane flexural wavenumber (Young's modulus stochastic), MCS with 10000 samples (blue diamond line) and present formulation (red star line) at discrete frequency

## 5. Elapsed time comparison

In the context of uncertainty quantification in periodic media, in crude MCS, the sample selection mainly depends on maximum number of simulations, elapsed time and desired accuracy. In order to establish the preeminence of SWFEM QEV over the WFEM MCS, the numerical costs involved in computation is compared with that of crude

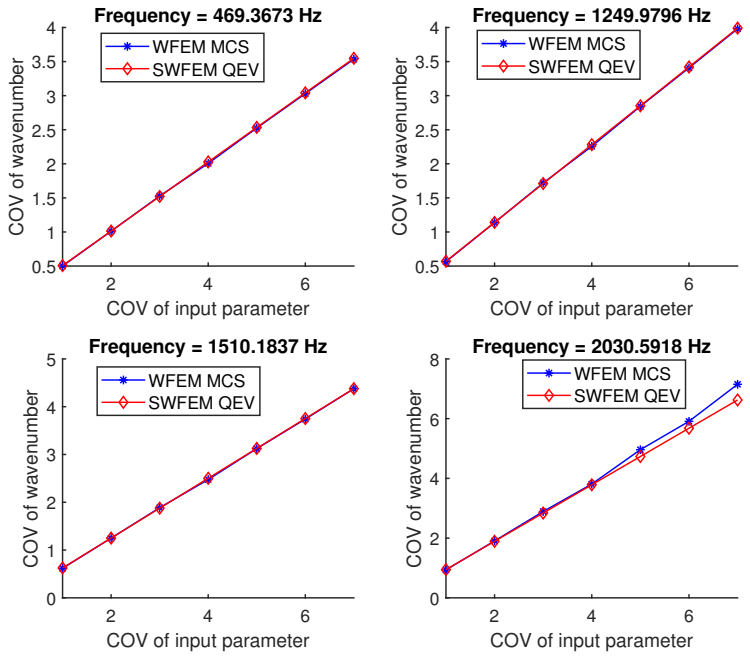


Figure 29: Variation of the out of plane flexural wavenumber (density stochastic), MCS with 10000 samples (blue star line) and present formulation (red diamond line) at discrete frequency

MCS with 10000 samples. As number of number of samples is increased the sampling error is decreased so 10000 sample are chosen in the reference results. One test case each for 1D and 2D cases are presented to exhibit the elapsed time comparison, because running many computations involving different parameter elapsed time trends are approximately equivalent in all cases. The test ran on the mobile workstation with the following characteristics, Intel Core$^{TM}$ i7 7820 HQ CPU@2.90GHz with 32 GB RAM. The comparison of elapsed time is reported in Table 5.

Table 5: Elapsed time comparison

| | WFEM MCS (10000 samples) | SWFEM QEV (single run) |
|---|---|---|
| 1D periodic media | 3840 seconds | 5.45 seconds |
| 2D periodic media | 14400 seconds | 21.57 seconds |

It can be seen from Table 5 that computational effort by application of SWFEM QEV is much smaller compared to WFEM MCS. The employed perturbation method computation efficiency results from the facts, to compute the response variability very few additional matrix factorisations are performed. The SWFEM QEV formulation uses the deterministic results to evaluate the response variability of the wavenumber. Thus, SWFEM QEV formulation has superiority over the WFEM MCS in computation cost, which can turn to great advantage for modeling complex

periodic structures.

## 6. Conclusion

This paper presents a computationally inexpensive stochastic spectral approach to study the uncertainties effects in 1D and 2D periodic media. In 1D cases, the proposed formulation applied to periodic rod and metamaterial rod on the frequency up to 2000 Hz. The comparison of present results is performed with SWFEM TM, WFEM MCS and analytical solutions. It provides excellent agreement and a substantial reduction in computation cost. The effect of uncertain parameters on the logitudinal wavenumber dispersion investigated considering stochasticity indicator and COV study. The effect on variation of longitudinal wavenumber is higher with elastic stochasticity than the stochastic density. Noteworthy, that in case of metamaterial rod system, the developed formulation can handle a higher level of uncertainties. In 2D cases, the formulation applied to homogeneous plate up to 10000 Hz and periodic plate with frequency up to 3000 Hz. In homogenous plate case, it is found that variation of out of plane flexural wavenumber is slightly higher with uncertain elasticity than the uncertain density. For periodic plate case, uncertainties affects the out of plane flexural wavenumber scattering, and maximum value of the variation of flexural wavenumber occurs at the band gap edge frequency. The COV study highlights the linear variation of flexural wavenumber in the low-frequency region and shifts to higher variation with increasing frequency. In terms of computation cost, developed formulation offers huge cost savings. The computational cost savings are very interesting and can be a good point for the optimisation and reliability study under uncertainties of complex periodic structures for damage detection and sensitivity analysis. Furthermore, The formulation can be employed for layered media, laminated, fibre reinforced and complicated cross-section geometry for determining the variation of dispersion properties, wavemodes, group and phase velocities.

## Acknowledgements

This project has received funding from the European Unions Horizon 2020 research and innovation programme under grant agreement No 675441.

## References

[1] Z. B. Cheng, Z. F. Shi, Y. L. Mo, Complex dispersion relations and evanescent waves in periodic beams via the extended differential quadrature method, Composite Structures 187 (January) (2018) 122–136. doi:10.1016/j.compstruct.2017.12.037.

[2] M. Syed, P. L. Bishay, Analysis and design of periodic beams for vibration attenuation, Journal of Vibration and control 0 (April) (2018) 1–12. doi:10.1177/1077546318774436.

[3] D. Yu, J. Wen, H. Zhao, Y. Liu, X. Wen, Vibration reduction by using the idea of phononic crystals in a pipe-conveying fluid, Journal of Sound and Vibration 318 (1-2) (2008) 193–205. doi:10.1016/j.jsv.2008.04.009.

[4] P. Wang, Q. Yi, C. Zhao, M. Xing, J. Tang, Wave propagation in periodic track structures: band-gap behaviours and formation mechanisms, Archive of Applied Mechanics 87 (3) (2017) 503–519. doi:10.1007/s00419-016-1207-8.

[5] M. S. Kushwaha, P. Halevi, G. Martínez, L. Dobrzynski, B. Djafari-Rouhani, Theory of acoustic band structure of periodic elastic composites, Physical Review B 49 (4) (1994) 2313–2322. doi:10.1103/PhysRevB.49.2313.

[6] Y. Tanaka, Y. Tomoyasu, S. I. Tamura, Band structure of acoustic waves in phononic lattices: Two-dimensional composites with large acoustic mismatch, Physical Review B - Condensed Matter and Materials Physics 62 (11) (2000) 7387–7392. doi:10.1103/PhysRevB.62.7387.

[7] I. Psarobas, N. Stefanou, A. Modinos, Scattering of elastic waves by periodic arrays of spherical bodies, Physical Review B - Condensed Matter and Materials Physics 62 (1) (2000) 278–291. arXiv:0004303, doi:10.1103/PhysRevB.62.278.

[8] J. M. Mencik, M. N. Ichchou, Multi-mode propagation and diffusion in structures through finite elements, European Journal of Mechanics, A/Solids 24 (5) (2005) 877–898. doi:10.1016/j.euromechsol.2005.05.004.

[9] H.-J. Xiang, Z.-F. Shi, Analysis of flexural vibration band gaps in periodic beams using differential quadrature method, Computers & Structures 87 (23-24) (2009) 1559–1566. doi:10.1016/J.COMPSTRUC.2009.07.009.
URL https://www.sciencedirect.com/science/article/pii/S0045794909002041?via{%}3Dihub

[10] J. Miles, One-Dimensional Stress-Wave Propagation in a Heterogeneous Medium, Journal of applied mech 33 (4) (1966) 11–12.

[11] C. R. Steele, Application of the wkb method in solid mechanics, in: S. Nemat-Nasser (Ed.), Mechanics Today, Vol. 3, Pergamon, 1976, Ch. 6, pp. 243–295. doi:10.1016/B978-0-08-019882-8.50013-X.

[12] C. Manohar, A. Keane, Axial vibration of a stochastic rod, Journal of Sound and Vibration 165 (2) (1993) 341–359.

[13] R. Langley, Wave transmission through one-dimensional near periodic structures: optimum and to random disorder, Journal of Sound and Vibration 188 (5) (1995) 717–743. doi:http://dx.doi.org/10.1006/jsvi.1995.0620.
URL http://www.sciencedirect.com/science/article/pii/S0022460X85706207

[14] J. P. Arenas, M. J. Crocker, A note on a WKB application to a duct of varying cross-section, Applied Mathematics Letters 14 (6) (2001) 667–671. doi:10.1016/S0893-9659(01)80024-0.

[15] A. Sarkar, R. Ghanem, Mid-frequency structural dynamics with parameter uncertainty, Computer Methods in Applied Mechanics and Engineering 191 (47-48) (2002) 5499–5513. doi:10.1016/S0045-7825(02)00465-6.

[16] M. N. Ichchou, F. Bouchoucha, M. A. Ben Souf, O. Dessombz, M. Haddar, Stochastic wave finite element for random periodic media through first-order perturbation, Computer Methods in Applied Mechanics and Engineering 200 (41-44) (2011) 2805–2813. doi:10.1016/j.cma.2011.05.004.
URL http://dx.doi.org/10.1016/j.cma.2011.05.004

[17] M. A. Ben Souf, O. Bareille, M. N. Ichchou, B. Troclet, M. Haddar, Variability of coupling loss factors through a wave finite element technique, Journal of Sound and Vibration 332 (9) (2013) 2179–2190. doi:10.1016/j.jsv.2012.07.003.
URL http://dx.doi.org/10.1016/j.jsv.2012.07.003

[18] M. A. Ben Souf, O. Bareille, M. N. Ichchou, F. Bouchoucha, M. Haddar, Waves and energy in random elastic guided media through the stochastic wave finite element method, Physics Letters, Section A: General, Atomic and Solid State Physics 377 (37) (2013) 2255–2264. doi:10.1016/j.physleta.2013.06.039.
URL http://dx.doi.org/10.1016/j.physleta.2013.06.039

[19] M. A. Ben Souf, M. Ichchou, O. Bareille, N. Bouhaddi, M. Haddar, Dynamics of random coupled structures through the wave finite element method, Engineering Computations 32 (7) (2015) 2020–2045. arXiv:/dx.doi.org/10.1108/BIJ-10-2012-0068, doi:http://dx.doi.org/10.1108/MRR-09-2015-0216.

[20] M. A. Ben Souf, O. Bareille, M. Ichchou, M. Haddar, The wave finite element method for uncertain systems with model uncertainty, Proceedings of the Institution of Mechanical Engineers, Part C: Journal of Mechanical Engineering Science 0 (0) (2015) 1–12. doi:10.1177/0954406215617197.
URL http://pic.sagepub.com/lookup/doi/10.1177/0954406215617197

[21] A. T. Fabro, N. S. Ferguson, T. Jain, R. Halkyard, B. R. Mace, Wave propagation in one-dimensional waveguides with slowly varying random spatially correlated variability, Journal of Sound and Vibration 343 (2015) 20–48. doi:10.1016/j.jsv.2015.01.013.
URL http://dx.doi.org/10.1016/j.jsv.2015.01.013

[22] J.-M. M. Mencik, D. Duhamel, A wave finite element-based approach for the modeling of periodic structures with local perturbations, Finite Elements in Analysis and Design 121 (15) (2016) 40–51. doi:10.1016/j.finel.2016.07.010.
URL http://dx.doi.org/10.1016/j.finel.2016.07.010

[23] A. T. Fabro, D. Beli, J. R. F. Arruda, N. Ferguson, B. R. Mace, Uncertainty analysis of band gaps for beams with periodically distributed resonators produced by additive manufacturing, in: Proceedings of ISMA2016, no. 1 in 27, 2016, pp. 2031–2042. doi:10.1037/a0033720.

[24] Y. Li, Y. Xu, Research on the effects of geometrical and material uncertainties on the band gap of the undulated beam, AIP ADVANCES 095315 (2017) 1–8.

[25] F. Bouchoucha, M. N. Ichchou, M. Haddar, Stochastic wave finite element method in uncertain elastic media through the second order perturbation, Journal of Applied Mechanics and Technical Physics 58 (2) (2017) 362–370. doi:10.1134/S0021894417020225.
URL http://link.springer.com/10.1134/S0021894417020225

[26] X.-F. Ma, T.-J. Li, Dynamic analysis of uncertain structures using an interval-wave approach, International Journal of Applied Mechanics 10 (2) (2018) 1–19. doi:10.1142/S1758825118500217.

[27] A. Fabro, N. Ferguson, B. Mace, Wave propagation in slowly varying waveguides using a finite element approach, Journal of Sound and Vibration 442 (2019) 308–329. doi:10.1016/j.jsv.2018.11.004.
URL https://linkinghub.elsevier.com/retrieve/pii/S0022460X18307569

[28] Y. Zhao, Y. Zhang, Symplectic Approach on the Wave Propagation Problem for periodic structures with uncertainty, Acta Mechanica Solida Sinicadoi:10.1007/s10338-019-00084-9.
URL https://doi.org/10.1007/s10338-019-00084-9

[29] M. A. Ben Souf, D. Chronopoulos, M. Ichchou, O. Bareille, M. Haddar, On the Variability of the Sound Transmission Loss of Composite Panels Through a Parametric Probabilistic Approach, Journal of Computational Acoustics 23 (2015) 1550018–1–23. doi:10.1142/S0218396X15500186.
URL http://www.worldscientific.com/doi/10.1142/S0218396X15500186

[30] L. Xie, B. Xia, G. Huang, J. Lei, J. Liu, Topology optimization of phononic crystals with uncertainties, Structural and Multidisciplinary Optimizationdoi:10.1007/s00158-017-1723-3.

[31] P. Zakian, N. Khaji, A stochastic spectral finite element method for wave propagation analyses with medium uncertainties, Applied Mathematical Modelling 63 (2018) 84–108. doi:10.1016/j.apm.2018.06.027.
URL https://doi.org/10.1016/j.apm.2018.06.027

[32] C. Droz, C. Zhou, M. N. Ichchou, J. P. Lainé, A hybrid wave-mode formulation for the vibro-acoustic analysis of 2D periodic structures, Journal of Sound and Vibration 363 (2016) 285–302. doi:10.1016/j.jsv.2015.11.003.
URL http://dx.doi.org/10.1016/j.jsv.2015.11.003

[33] Y. Waki, B. R. Mace, M. J. Brennan, Numerical issues concerning the wave and finite element method for free and forced vibrations of waveguides, Journal of Sound and Vibration 327 (1-2) (2009) 92–108. doi:10.1016/j.jsv.2009.06.005.
URL http://dx.doi.org/10.1016/j.jsv.2009.06.005

[34] D. J. Mead, A general theory of harmonic wave propagation in linear periodic systems with multiple coupling, Journal of Sound and Vibration 27 (2) (1973) 235–260. doi:10.1016/0022-460X(73)90064-3.

[35] L. Houillon, M. N. Ichchou, L. Jezequel, Wave motion in thin-walled structures, Journal of Sound and Vibration 281 (3-5) (2005) 483–507. arXiv:ISSN:0022460X, doi:10.1016/j.jsv.2004.01.020.

[36] E. D. Nobrega, F. Gautier, A. Pelat, J. M. Dos Santos, Vibration band gaps for elastic metamaterial rods using wave finite element method, Mechanical Systems and Signal Processing 79 (2016) 192–202. doi:10.1016/j.ymssp.2016.02.059.
URL http://dx.doi.org/10.1016/j.ymssp.2016.02.059

[37] B. R. Mace, E. Manconi, Modelling wave propagation in two-dimensional structures using finite element analysis, Journal of Sound and Vibration 318 (4-5) (2008) 884–902. doi:10.1016/j.jsv.2008.04.039.

[38] B. Tian, B. Tie, D. Aubry, X. Su, Elastic Wave Propagation in Periodic Cellular Structures, Computer Modeling in Science and Engineering

76 (4) (2011) 217–233.
URL http://www.techscience.com/doi/10.3970/cmes.2011.076.217.pdf

## A. Derivation for the standard deviation of the eigenvalues and eigenvectors for 1D periodic media

Stochastic eigenvalues ($\widetilde{\mu_i}$) and stochastic eigenvectors $\left(\widetilde{\Phi}_q\right)_i$ are the solution of the stochastic quadratic equation Eq. (5). The zeroth order chaos expansion of Eq. (5) leads to

$$\left(\overline{D}_{RL} + \overline{\mu}_i I_{2n}(\overline{D}_{LL} + \overline{D}_{RR}) + \overline{\mu}_i^2 I_{2n}\overline{D}_{LR}\right)\left(\overline{\Phi}_q\right)_i = 0 \tag{A.1}$$

The first order chaos expansion of the stochastic quadratic Eq. (5) leads to

$$\begin{aligned}\left[\overline{D}_{RL} + \overline{\mu}_i I_{2n}(\overline{D}_{LL} + \overline{D}_{RR}) + \overline{\mu}_i^2 I_{2n}\overline{D}_{LR}\right]\sigma_{\left(\Phi_{qL}\right)_i} \\ + \left[\sigma_{D_{RL}} + \sigma_{\mu_i} I_{2n}(\overline{D}_{LL} + \overline{D}_{RR}) + \overline{\mu}_i I_{2n}(\sigma_{D_{LL}} + \sigma_{D_{RR}} + 2\overline{\mu}_i I_{2n}\sigma_{\mu_i}\overline{D}_{LR} + \overline{\mu}_i^2 I_{2n}\sigma_{D_{LR}})\right]\left(\overline{\Phi}_q\right)_i = 0\end{aligned} \tag{A.2}$$

From above equation the standard deviation of eigenvectors $\sigma_{\left(\Phi_q\right)_i}$ can be expressed as

$$\begin{aligned}\sigma_{\left(\Phi_q\right)_i} = -\left[\overline{D}_{RL} + \overline{\mu}_i I_{2n}(\overline{D}_{LL} + \overline{D}_{RR}) + \overline{\mu}_i^2 I_{2n}\overline{D}_{LR}\right]^{-1} \\ \left[\sigma_{D_{RL}} + \sigma_{\mu_i I_{2n}}(\overline{D}_{LL} + \overline{D}_{RR}) + \overline{\mu}_i I_{2n}\left(\sigma_{D_{LL}} + \sigma_{D_{RR}}\right) + 2\overline{\mu}_i I_{2n}\sigma_{\mu_i}\overline{D}_{LR} + \overline{\mu}_i^2 I_{2n}\sigma_{D_{LR}}\right]\left(\overline{\Phi}_q\right)_i\end{aligned} \tag{A.3}$$

$\left(\widetilde{\Phi}_q\right)_i^T$, the stochastic left eigenvectors linked with stochastic left eigenvalues $\widetilde{\mu}_i^{-1}$, which form the stochastic left quadratic eigenvalue problem as

$$\left(\widetilde{\Phi}_q\right)_i^T\left(\widetilde{D}_{RL} + \widetilde{\mu}_i^{-1} I_{2n}(\widetilde{D}_{LL} + \widetilde{D}_{RR}) + \widetilde{\mu}_i^{-2} I_{2n}\widetilde{D}_{LR}\right) = 0 \tag{A.4}$$

The first order chaos expansion of stochastic left quadratic eigenvalue leads to

$$\begin{aligned}\sigma_{\left(\Phi_q\right)_i}{}^T\left[\overline{D}_{RL} + \overline{\mu}_i{}^{-1} I_{2n}(\overline{D}_{LL} + \overline{D}_{RR}) + \overline{\mu}_i{}^{-2} I_{2n}\overline{D}_{LR}\right] + \left(\overline{\Phi}_q\right)_i^T\left[\sigma_{D_{RL}} - \overline{\mu}_i{}^{-2} I_{2n}\sigma_{\mu_i}(\overline{D}_{LL} + \overline{D}_{RR})\right. \\ \left. + \overline{\mu}_i{}^{-1} I_{2n}(\sigma_{D_{LL}} + \sigma_{D_{RR}}) - 2\overline{\mu}_i{}^{-3} I_{2n}\sigma_{\mu_i}\overline{D}_{LR} + \overline{\mu}_i{}^{-2} I_{2n}\sigma_{DR}\right] = 0\end{aligned} \tag{A.5}$$

In the above equation, identification of the targeted terms $\sigma_{\left(\Phi_q\right)_i}, \sigma_{\mu_i}$ and replacement of $\sigma_{\left(\Phi_q\right)_i}$ leads to

$$\begin{aligned}-\Big[\ \left[\overline{D}_{RL} + \overline{\mu}_i I_{2n}(\overline{D}_{LL} + \overline{D}_{RR}) + \overline{\mu}_i^2 I_{2n}\overline{D}_{LR}\right]^{-1}\left[\sigma_{D_{RL}} + \sigma_{\mu_i} I_{2n}(\overline{D}_{LL} + \overline{D}_{RR}) + \overline{\mu}_i I_{2n}(\sigma_{D_{LL}} + \sigma_{D_{RR}})\right. \\ \left. + 2\overline{\mu}_i\sigma_{\mu_i} I_{2n}\overline{D}_{LR} + \overline{\mu}_i^2 I_{2n}\sigma_{D_{LR}}](\overline{\Phi}_q)_i\right]^T\left[\overline{D}_{RL} + \overline{\mu}_i{}^{-1} I_{2n}(\overline{D}_{LL} + \overline{D}_{RR}) + \overline{\mu}_i{}^{-2} I_{2n}\overline{D}_{LR}\right] + \left(\overline{\Phi}_q\right)_i^T \\ \left[\sigma_{D_{RL}} - \overline{\mu}_i^{-2} I_{2n}\sigma_{\mu_i}(\overline{D}_{LL} + \overline{D}_{RR}) + \mu_i^{-1} I_{2n}(\sigma_{D_{LL}} + \sigma_{D_{RR}}) - 2\mu_i^{-3} I_{2n}\sigma_{\mu_i} D_{LR} + \mu_i^{-2} I_{2n}\sigma_{D_{LR}}\right] = 0\end{aligned} \tag{A.6}$$

Simplification of the above equation for $\sigma_{\mu_i}$ leads to

$$\begin{aligned}\sigma_{\mu_i} I_{2n}\left[\left(\overline{\Phi}_q\right)_i^T\left[-(\overline{D}_{LL} + \overline{D}_{RR})^T - 2\overline{\mu}_i I_{2n}\overline{D}_{LR}^T\right]\left[\overline{D}_{RL} + \mu_i I_{2n}(\overline{D}_{LL} + \overline{D}_{RR}) + \overline{\mu}_i^2 I_{2n}\overline{D}_{LR}\right]^{-1}\right. \\ \left.\left[\overline{D}_{RL} + \overline{\mu}_i^{-1} I_{2n}(\overline{D}_{LL} + \overline{D}_{RR}) + \overline{\mu}_i^{-2} I_{2n}\overline{D}_{LR}\right] - \left(\Phi_q\right)_i^T\left[\overline{\mu}_i^{-2} I_{2n}(\overline{D}_{LL} + \overline{D}_{RR}) + 2\overline{\mu}_i^{-3} I_{2n}\overline{D}_{LR}\right]\right] \\ = \left(\overline{\Phi}_q\right)_i^T\left[\sigma_{D_{RL}}^T + \overline{\mu}_i I_{2n}\left(\sigma_{D_{LL}} + \sigma_{D_{RR}}\right)^T + \overline{\mu}_i^2 I_{2n}\sigma_{D_{LR}}^T\right]\left[\overline{D}_{RL} + \overline{\mu}_i I_{2n}\left(\overline{D}_{LL} + \overline{D}_{RR}\right) + \overline{\mu}_i^2 I_{2n}\overline{D}_{LR}\right]^{-1} \\ \left[\overline{D}_{RL} + \overline{\mu}_i^{-1} I_{2n}\left(\overline{D}_{LL} + \overline{D}_{RR}\right) + \overline{\mu}_i^{-2} I_{2n}\overline{D}_{LR}\right] - \left(\overline{\Phi}_q\right)_i^T\left[\sigma_{D_{RL}} + \overline{\mu}_i^{-1} I_{2n}\left(\sigma_{D_{LL}} + \sigma_{D_{RR}}\right) + \overline{\mu}_i^{-2}\sigma_{D_{LR}}\right]\end{aligned} \tag{A.7}$$

Finally, the analytical expression for the standard deviation of the eigenvalues $\left(\sigma_{\mu_i}\right)$ is

$$\begin{aligned}\sigma_{\mu_i} = \left(\overline{\Phi}_q\right)_i^T &\left[\sigma_{D_{RL}}^T + \overline{\mu}_i I_{2n}\left(\sigma_{D_{LL}} + \sigma_{D_{RR}}\right)^T + \overline{\mu}_i^2 I_{2n}\sigma_{D_{LR}}^T\right]\left[\overline{D}_{RL} + \overline{\mu}_i I_{2n}(\overline{D}_{LL} + \overline{D}_{RR}) + \overline{\mu}_i^2 I_{2n}\overline{D}_{LR}\right]^{-1} \\ &\left[\overline{D}_{RL} + \overline{\mu}_i{}^{-1} I_{2n}(\overline{D}_{LL} + \overline{D}_{RR}) + \overline{\mu}_i{}^{-2} I_{2n}\overline{D}_{LR}\right] - \left(\overline{\Phi}_q\right)_i^T\left[\sigma_{D_{RL}} + \overline{\mu}_i{}^{-1} I_{2n}\left(\sigma_{D_{LL}} + \sigma_{D_{RR}}\right) + \overline{\mu}_i{}^{-2} I_{2n}\sigma_{D_{LR}}\right] \\ &\left[\left(\overline{\Phi}_q\right)_i^T\left[-(\overline{D}_{LL} + \overline{D}_{RR})^T - 2\overline{\mu}_i I_{2n}\overline{D}_{LR}^T\right]\left[\overline{D}_{RL} + \overline{\mu}_i I_{2n}(\overline{D}_{LL} + \overline{D}_{RR}) + \overline{\mu}_i^2 I_{2n}\overline{D}_{LR}\right]^{-1}\right. \\ &\left.\left[\overline{D}_{RL} + \overline{\mu}_i{}^{-1} I_{2n}(\overline{D}_{LL} + \overline{D}_{RR}) + \overline{\mu}_i{}^{-2} I_{2n}\overline{D}_{LR}\right] - \left(\overline{\Phi}_q\right)_i^T\left[\overline{\mu}_i{}^{-2} I_{2n}(\overline{D}_{LL} + \overline{D}_{RR}) + 2\overline{\mu}_i{}^{-3} I_{2n}\overline{D}_{LR}\right]\right]^{-1}\end{aligned} \tag{A.8}$$

Also the analytical expression for the standard deviation of the eigenvectors $\left(\sigma_{(\Phi_q)_i}\right)$ is

$$\begin{aligned}\sigma_{(\Phi_q)_i} = -&\left[\overline{D}_{RL} + \overline{\mu}_i I_{2n}(\overline{D}_{LL} + \overline{D}_{RR}) + \overline{\mu}_i^2 I_{2n}\overline{D}_{LR}\right]^{-1} \\ &\left[\sigma_{D_{RL}} + \sigma_{\mu_i I_{2n}}(\overline{D}_{LL} + \overline{D}_{RR}) + \overline{\mu}_i I_{2n}\left(\sigma_{D_{LL}} + \sigma_{D_{RR}}\right) + 2\overline{\mu}_i\sigma_{\mu_i} I_{2n}\overline{D}_{LR} + \overline{\mu}_i^2 I_{2n}\sigma_{D_{LR}}\right]\left(\overline{\Phi}_q\right)_i\end{aligned} \tag{A.9}$$

Eq. (A.8) and Eq. (A.9) are the the explicit expressions for the statistical characterization of the wavenumber using deterministic eigenvalue solutions in the 1D periodic media.

## B. Derivation for the standard deviation of the condensed dynamic stiffness matrix for 1D periodic media

The dynamic condensation and first order expansion of Eq. (9) leads to

$$\sigma_D = \begin{bmatrix} \sigma_{D_{LL}} & \sigma_{D_{LR}} \\ \sigma_{D_{RL}} & \sigma_{D_{RR}} \end{bmatrix} \tag{B.1}$$

where

$$\begin{aligned}\sigma_{D_{LL}} &= \sigma_{\widehat{D}_{LL}} - \overline{\widehat{D}}_{LI}\overline{\widehat{D}}_{II}{}^{-1}\sigma_{\widehat{D}_{IL}} + \overline{\widehat{D}}_{LI}\overline{\widehat{D}}_{II}{}^{-2}\sigma_{\widehat{D}_{II}}\overline{\widehat{D}}_{IL} - \sigma_{\widehat{D}_{LI}}\overline{\widehat{D}}_{II}{}^{-1}\overline{\widehat{D}}_{IL} \\ \sigma_{D_{LR}} &= \sigma_{\widehat{D}_{LR}} - \overline{\widehat{D}}_{LI}\overline{\widehat{D}}_{II}{}^{-1}\sigma_{\widehat{D}_{IR}} + \overline{\widehat{D}}_{LI}\overline{\widehat{D}}_{II}{}^{-2}\sigma_{\widehat{D}_{II}}\overline{\widehat{D}}_{IR} - \sigma_{\widehat{D}_{LI}}\overline{\widehat{D}}_{II}{}^{-1}\overline{\widehat{D}}_{IR} \\ \sigma_{D_{RL}} &= \sigma_{\widehat{D}_{RL}} - \overline{\widehat{D}}_{RI}\overline{\widehat{D}}_{II}{}^{-1}\sigma_{\widehat{D}_{IL}} + \overline{\widehat{D}}_{RI}\overline{\widehat{D}}_{II}{}^{-2}\sigma_{\widehat{D}_{II}}\overline{\widehat{D}}_{IL} - \sigma_{\widehat{D}_{RI}}\overline{\widehat{D}}_{II}{}^{-1}\overline{\widehat{D}}_{IL} \\ \sigma_{D_{RR}} &= \sigma_{\widehat{D}_{RR}} - \overline{\widehat{D}}_{RI}\overline{\widehat{D}}_{II}{}^{-1}\sigma_{\widehat{D}_{IR}} + \overline{\widehat{D}}_{RI}\overline{\widehat{D}}_{II}{}^{-2}\sigma_{\widehat{D}_{II}}\overline{\widehat{D}}_{IR} - \sigma_{\widehat{D}_{RI}}\overline{\widehat{D}}_{II}{}^{-1}\overline{\widehat{D}}_{IR}\end{aligned}$$

Above expressions are organized in the matrix form as

$$\sigma_D = \begin{bmatrix} \sigma_{\widehat{D}_{LL}} & \sigma_{\widehat{D}_{LR}} \\ \sigma_{\widehat{D}_{RL}} & \sigma_{\widehat{D}_{RR}} \end{bmatrix} - \begin{bmatrix} \overline{\widehat{D}}_{LI} & \sigma_{\widehat{D}_{LI}} \\ \overline{\widehat{D}}_{RI} & \sigma_{\widehat{D}_{RI}} \end{bmatrix}\begin{bmatrix} \overline{\widehat{D}}_{II}{}^{-1} & -\overline{\widehat{D}}_{II}{}^{-2}\sigma_{\widehat{D}_{II}} \\ 0 & \overline{\widehat{D}}_{II}{}^{-1} \end{bmatrix}\begin{bmatrix} \sigma_{\widehat{D}_{IL}} & \sigma_{\widehat{D}_{IR}} \\ \overline{\widehat{D}}_{IL} & \overline{\widehat{D}}_{IR} \end{bmatrix} \tag{B.2}$$

To simplify the computation, standard deviation of the condensed dynamic stiffness matrix is

$$\sigma_D = \begin{bmatrix} \sigma_{\widehat{D}_{LL}} & \sigma_{\widehat{D}_{LR}} \\ \sigma_{\widehat{D}_{RL}} & \sigma_{\widehat{D}_{RR}} \end{bmatrix} - \begin{bmatrix} \overline{\widehat{D}}_{LI} & \sigma_{\widehat{D}_{LI}} \\ \overline{\widehat{D}}_{RI} & \sigma_{\widehat{D}_{RI}} \end{bmatrix}\begin{bmatrix} \overline{\widehat{D}}_{II}{}^{-1} & -\overline{\widehat{D}}_{II}{}^{-1}\sigma_{\widehat{D}_{II}}\overline{\widehat{D}}_{II}{}^{-1} \\ 0 & \overline{\widehat{D}}_{II}{}^{-1} \end{bmatrix}\begin{bmatrix} \sigma_{\widehat{D}_{IL}} & \sigma_{\widehat{D}_{IR}} \\ \overline{\widehat{D}}_{IL} & \overline{\widehat{D}}_{IR} \end{bmatrix} \tag{B.3}$$

where symbol $\overline{\widehat{(.)}}$ represents the mean value from the original dynamic stiffness matrix.

## C. Derivation for the standard deviation of the eigenvalues and eigenvectors for 2D periodic media

The first order chaos expansion of stochastic spectral problem in Eq. (22) leads to

$$\Big[(\overline{D}_{21}+\overline{D}_{43}+\overline{D}_{41}\lambda_y^{-1}+\overline{D}_{23}\lambda_y)+\overline{\mu}_i I_{2n}(\overline{D}_{11}+\overline{D}_{22}+\overline{D}_{33}+\overline{D}_{44}+(\overline{D}_{31}+\overline{D}_{42})\lambda_y^{-1}+(\overline{D}_{13}+\overline{D}_{24})\lambda_y)$$
$$+\overline{\mu}_i^2 I_{2n}(\overline{D}_{12}+\overline{D}_{34}+\overline{D}_{32}\lambda_y^{-1}+\overline{D}_{14}\lambda_y)\Big]\sigma_{(\Phi_q)_i}+\Big[(\sigma_{D_{21}}+\sigma_{D_{43}}+\sigma_{D_{41}}\lambda_y^{-1}+\sigma_{D_{23}}\lambda_y)+\sigma_{\mu_i I_{2n}}(\overline{D}_{11}+\overline{D}_{22}$$
$$+\overline{D}_{33}+\overline{D}_{44}+(\overline{D}_{31}+\overline{D}_{42})\lambda_y^{-1}+(\overline{D}_{13}+\overline{D}_{24})\lambda_y)+\overline{\mu}_i I_{2n}(\sigma_{D_{11}}+\sigma_{D_{22}}+\sigma_{D_{33}}+\sigma_{D_{44}}+\sigma_{D_{31}}\lambda_y^{-1}$$
$$+\sigma_{D_{42}}\lambda_y^{-1}+\sigma_{D_{13}}\lambda_y+\sigma_{D_{24}}\lambda_y)+2\overline{\mu}_i I_{2n}\sigma_{\mu_i}(\overline{D}_{12}+\overline{D}_{34}+\overline{D}_{32}\lambda_y^{-1}+\overline{D}_{14}\lambda_y)+\overline{\mu}_i^2 I_{2n}(\sigma_{D_{12}}+\sigma_{D_{34}}$$
$$+\sigma_{D_{32}}\lambda_y^{-1}+\sigma_{D_{14}}\lambda_y)\Big]\left(\overline{\Phi}_q\right)_i=0 \quad \text{(C.1)}$$

From above equation the standard deviation of the eigenvectors is

$$\sigma_{(\Phi_q)_i}=-\Big[(\sigma_{D_{21}}+\sigma_{D_{43}}+\sigma_{D_{41}}\lambda_y^{-1}+\sigma_{D_{23}}\lambda_y)+\sigma_{\mu_i}I_{2n}(\overline{D}_{11}+\overline{D}_{22}+\overline{D}_{33}+\overline{D}_{44}+(\overline{D}_{31}+\overline{D}_{42})\lambda_y^{-1}$$
$$+(\overline{D}_{13}+\overline{D}_{24})\lambda_y)+\overline{\mu}_i I_{2n}(\sigma_{D_{11}}+\sigma_{D_{22}}+\sigma_{D_{33}}+\sigma_{D_{44}}+\sigma_{D_{31}}\lambda_y^{-1}+\sigma_{D_{42}}\lambda_y^{-1}+\sigma_{D_{13}}\lambda_y+\sigma_{D_{24}}\lambda_y)$$
$$+2\overline{\mu}_i I_{2n}\sigma_{\mu_i}(\overline{D}_{12}+\overline{D}_{34}+\overline{D}_{32}\lambda_y^{-1}+\overline{D}_{14}\lambda_y)+\overline{\mu}_i^2 I_{2n}(\sigma_{D_{12}}+\sigma_{D_{34}}+\sigma_{D_{32}}\lambda_y^{-1}+\sigma_{D_{14}}\lambda_y)\Big]\left(\overline{\Phi}_q\right)_i\Big[(\overline{D}_{21}$$
$$+\overline{D}_{43}+\overline{D}_{41}\lambda_y^{-1}+\overline{D}_{23}\lambda_y)+\overline{\mu}_i I_{2n}(\overline{D}_{11}+\overline{D}_{22}+\overline{D}_{33}+\overline{D}_{44}+(\overline{D}_{31}+\overline{D}_{42})\lambda_y^{-1}+(\overline{D}_{13}+\overline{D}_{24})\lambda_y)$$
$$+\overline{\mu}_i^2 I_{2n}(\overline{D}_{12}+\overline{D}_{34}+\overline{D}_{32}\lambda_y^{-1}+\overline{D}_{14}\lambda_y)\Big]^{-1} \quad \text{(C.2)}$$

$\left(\widetilde{\Phi}_q\right)_i^T$, the left stochastic eigenvectors linked with stochastic left eigenvalues $\widetilde{\mu}_i^{-1}$, which form the stochastic left quadratic eigenvalue problem as

$$\left(\Phi_q\right)_i^T\Big[(\widetilde{D}_{21}+\widetilde{D}_{43}+\widetilde{D}_{41}\lambda_y^{-1}+\widetilde{D}_{23}\lambda_y)+\widetilde{\mu}_i^{-1}I_{2n}(\widetilde{D}_{11}+\widetilde{D}_{22}+\widetilde{D}_{33}+\widetilde{D}_{44}+(\widetilde{D}_{31}+\widetilde{D}_{42})\lambda_y^{-1}$$
$$+(\widetilde{D}_{13}+\widetilde{D}_{24})\lambda_y)+\widetilde{\mu}_i^{-2}I_{2n}(\widetilde{D}_{12}+\widetilde{D}_{34}+\widetilde{D}_{32}\lambda_y^{-1}+\widetilde{D}_{14}\lambda_y)\Big]=0 \quad \text{(C.3)}$$

First order chaos expansion of the stochastic left eigenvalue problem leads to

$$\sigma_{(\Phi_q)_i}{}^T\Big[(\overline{D}_{21}+\overline{D}_{43}+\overline{D}_{41}\lambda_y^{-1}+\overline{D}_{23}\lambda_y)+\overline{\mu}_i{}^{-1}I_{2n}(\overline{D}_{11}+\overline{D}_{22}+\overline{D}_{33}+\overline{D}_{44}+(\overline{D}_{31}+\overline{D}_{42})\lambda_y^{-1}+(\overline{D}_{13}+\overline{D}_{24})\lambda_y)$$
$$+\overline{\mu}_i{}^{-2}I_{2n}(\overline{D}_{12}+\overline{D}_{34}+\overline{D}_{32}\lambda_y^{-1}+\overline{D}_{14}\lambda_y)\Big]+\left(\Phi_q\right)_i^T\Big[(\sigma_{D_{21}}+\sigma_{D_{43}}+\sigma_{D_{41}}\lambda_y^{-1}+\sigma_{D_{23}}\lambda_y)-\overline{\mu}_i{}^{-2}I_{2n}\sigma_{\mu_i}(\overline{D}_{11}+\overline{D}_{22}$$
$$+\overline{D}_{33}+\overline{D}_{44}+(\overline{D}_{31}+\overline{D}_{42})\lambda_y\Big)+\overline{\mu}_i{}^{-1}I_{2n}(\sigma_{D_{11}}+\sigma_{D_{22}}+\sigma_{D_{33}}+\sigma_{D_{44}}+\sigma_{D_{31}}\lambda_y^{-1}+\sigma_{D_{42}}\lambda_y^{-1}+\sigma_{D_{13}}\lambda_y+\sigma_{D_{24}}\lambda_y)$$
$$-2\overline{\mu}_i{}^{-3}I_{2n}\sigma_{\mu_i}(\overline{D}_{12}+\overline{D}_{34}+\overline{D}_{32}\lambda_y^{-1}+\overline{D}_{14}\lambda_y)+\overline{\mu}_i{}^{-2}I_{2n}(\sigma_{D_{12}}+\sigma_{D_{34}}+\sigma_{D_{32}}\lambda_y^{-1}+\sigma_{D_{14}}\lambda_y)\Big]=0 \quad \text{(C.4)}$$

Inserting $\sigma_{(\Phi_q)_i}$ in the above equation and simplification leads to the standard deviation of the eigenvalue as

$$\sigma_{\mu_i} = \left(\overline{\Phi}_q\right)_i^T \left[(\sigma_{D_{21}}^T + \sigma_{D_{43}}^T + (\sigma_{D_{41}}\lambda_y^{-1})^T + (\sigma_{D_{23}}\lambda_y)^T) + \overline{\mu}_i I_{2n}(\sigma_{D_{11}}^T + \sigma_{D_{22}}^T + \sigma_{D_{33}}^T + \sigma_{D_{44}}^T + (\sigma_{D_{31}}\lambda_y^{-1})^T + (\sigma_{D_{42}}\lambda_y^{-1})^T \right.$$
$$\left. +(\sigma_{D_{13}}\lambda_y)^T + (\sigma_{D_{24}}\lambda_y)^T) + \overline{\mu}_i^2 I_{2n}(\sigma_{D_{12}}^T + \sigma_{D_{34}}^T + (\sigma_{D_{32}}\lambda_y^{-1})^T + (\sigma_{D_{14}}\lambda_y)^T)\right] \left[(\overline{D}_{21}^T + \overline{D}_{43}^T + (\overline{D}_{41}\lambda_y^{-1})^T + (\overline{D}_{23}\lambda_y)^T)\right.$$
$$\left. + \sigma_{\mu_i} I_{2n}(\overline{D}_{11}^T + \overline{D}_{22}^T + \overline{D}_{33}^T + \overline{D}_{44}^T + ((\overline{D}_{31} + \overline{D}_{42})\lambda_y^{-1})^T + ((\overline{D}_{13} + \overline{D}_{24})\lambda_y)^T) + \overline{\mu}_i^2 I_{2n}(\overline{D}_{12}^T + \overline{D}_{34}^T + (\overline{D}_{32}\lambda_y^{-1})^T + (\overline{D}_{14}\lambda_y)^T\right]^{-1}$$
$$+ \left[(\overline{D}_{21} + \overline{D}_{43} + (\overline{D}_{41}\lambda_y^{-1})(\overline{D}_{23}\lambda_y)) + \overline{\mu}_i{}^{-1} I_{2n}(\overline{D}_{11} + \overline{D}_{22} + \overline{D}_{33} + \overline{D}_{44} + (\overline{D}_{31} + \overline{D}_{42})\lambda_y^{-1} + (\overline{D}_{13} + \overline{D}_{24})\lambda_y)\right.$$
$$\left. +\overline{\mu}_i{}^{-2} I_{2n}(\overline{D}_{12} + \overline{D}_{34} + \overline{D}_{32}\lambda_y^{-1} + \overline{D}_{14}\lambda_y)\right] - \left(\overline{\Phi}_q\right)_i^T \left[(\sigma_{D_{21}} + \sigma_{D_{43}} + \sigma_{D_{41}}\lambda_y^{-1} + \sigma_{D_{23}}\lambda_y) + \overline{\mu}_i{}^{-1} I_{2n}(\sigma_{D_{11}} + \sigma_{D_{22}} + \sigma_{D_{33}}\right.$$
$$\left. +\sigma_{D_{44}} + \sigma_{D_{31}}\lambda_y^{-1} + \sigma_{D_{42}}\lambda_y^{-1} + \sigma_{D_{13}}\lambda_y + \sigma_{D_{24}}\lambda_y) + \overline{\mu}_i{}^{-2} I_{2n}\left(\sigma_{D_{12}} + \sigma_{D_{34}} + \sigma_{D_{32}}\lambda_y^{-1} + \sigma_{D_{14}}\lambda_y\right)\right]$$
$$\left[\left(\overline{\Phi}_q\right)_i^T \left[-(\overline{D}_{11}^T + \overline{D}_{22}^T + \overline{D}_{33}^T + \overline{D}_{44}^T + (\overline{D}_{31}\lambda_y^{-1})^T + (\overline{D}_{42}\lambda_y^{-1})^T) - 2\overline{\mu}_i I_{2n}(\overline{D}_{12}^T + \overline{D}_{34}^T + (\overline{D}_{32}\lambda_y^{-1})^T + (\overline{D}_{14}\lambda_y)^T)\right]\right.$$
$$\left[(\overline{D}_{21}^T + \overline{D}_{43}^T + (\overline{D}_{41}\lambda_y^{-1})^T + (\overline{D}_{23}\lambda_y)^T) + \overline{\mu}_i I_{2n}(\overline{D}_{11}^T + \overline{D}_{22}^T + \overline{D}_{33}^T + \overline{D}_{44}^T + ((\overline{D}_{31} + \overline{D}_{42})\lambda_y^{-1})^T + (\overline{D}_{13} + \overline{D}_{24})\lambda_y^T)\right.$$
$$\left. +\overline{\mu}_i^2 I_{2n}(\overline{D}_{12}^T + \overline{D}_{34}^T + (\overline{D}_{32}\lambda_y^{-1})^T + (\overline{D}_{14}\lambda_y))^T\right]^{-1} \left[(\overline{D}_{21} + \overline{D}_{43} + (\overline{D}_{41}\lambda_y^{-1}) + (\overline{D}_{23}\lambda_y)) + \overline{\mu}_i{}^{-1} I_{2n}(\overline{D}_{11} + \overline{D}_{22} + \overline{D}_{33}\right.$$
$$\left. +\overline{D}_{44} + (\overline{D}_{31} + \overline{D}_{42})\lambda_y^{-1} + (\overline{D}_{13} + \overline{D}_{24})\lambda_y) + \overline{\mu}_i{}^{-2} I_{2n}(\overline{D}_{12} + \overline{D}_{34} + \overline{D}_{32}\lambda_y^{-1} + \overline{D}_{14}\lambda_y)\right] - \left(\overline{\Phi}_q\right)_i^T$$
$$\left.\left[\overline{\mu}_i{}^{-2} I_{2n}(\overline{D}_{11} + \overline{D}_{22} + \overline{D}_{33} + \overline{D}_{44} + (\overline{D}_{31} + \overline{D}_{42})\lambda_y^{-1} + (\overline{D}_{13} + \overline{D}_{24})\lambda_y) + 2\overline{\mu}_i{}^{-3} I_{2n}(\overline{D}_{12} + \overline{D}_{34} + \overline{D}_{32}\lambda_y^{-1} + \overline{D}_{14}\lambda_y)\right]\right]^{-1} \tag{C.5}$$

The explicit expression for the standard deviation of the eigvenvectors is

$$\sigma_{(\Phi_q)_i} = -\left[(\sigma_{D_{21}} + \sigma_{D_{43}} + \sigma_{D_{41}}\lambda_y^{-1} + \sigma_{D_{23}}\lambda_y) + \sigma_{\mu_i} I_{2n}(\overline{D}_{11} + \overline{D}_{22} + \overline{D}_{33} + \overline{D}_{44} + (\overline{D}_{31} + \overline{D}_{42})\lambda_y^{-1}\right.$$
$$+(\overline{D}_{13} + \overline{D}_{24})\lambda_y) + \overline{\mu}_i I_{2n}(\sigma_{D_{11}} + \sigma_{D_{22}} + \sigma_{D_{33}} + \sigma_{D_{44}} + \sigma_{D_{31}}\lambda_y^{-1} + \sigma_{D_{42}}\lambda_y^{-1} + \sigma_{D_{13}}\lambda_y + \sigma_{D_{24}}\lambda_y)$$
$$\left. +2\overline{\mu}_i I_{2n}\sigma_{\mu_i}(\overline{D}_{12} + \overline{D}_{34} + \overline{D}_{32}\lambda_y^{-1} + \overline{D}_{14}\lambda_y) + \overline{\mu}_i^2 I_{2n}(\sigma_{D_{12}} + \sigma_{D_{34}} + \sigma_{D_{32}}\lambda_y^{-1} + \sigma_{D_{14}}\lambda_y)\right]\left(\overline{\Phi}_q\right)_i$$
$$\left[(\overline{D}_{21} + \overline{D}_{43} + \overline{D}_{41}\lambda_y^{-1} + \overline{D}_{23}\lambda_y) + \overline{\mu}_i I_{2n}(\overline{D}_{11} + \overline{D}_{22} + \overline{D}_{33} + \overline{D}_{44} + (\overline{D}_{31} + \overline{D}_{42})\lambda_y^{-1} + (\overline{D}_{13} + \overline{D}_{24})\lambda_y)\right.$$
$$\left. + \overline{\mu}_i^2 I_{2n}(\overline{D}_{12} + \overline{D}_{34} + \overline{D}_{32}\lambda_y^{-1} + \overline{D}_{14}\lambda_y)\right]^{-1} \tag{C.6}$$

Above Eq. (C.5) and Eq. (C.6) are the explicit expressions for the statistics of wave propagation using deterministic eigenvalue solutions in the periodic media for the 2D cases.

## D. Derivation for the standard deviation of the condensed dynamic stiffness matrix for 2D periodic media

The dynamic stiffness matrix from Eq. (26) is in the following form

$$D = \begin{bmatrix} \widehat{D}_{bdbd} & \widehat{D}_{bdI} \\ \widehat{D}_{Ibd} & \widehat{D}_{II} \end{bmatrix} \tag{D.1}$$

where symbol $\widehat{(.)}$ represents the elements from the original dynamic stiffness matrix. The dynamic equation of motion can be written as

$$\begin{bmatrix} \widehat{D}_{bdbd} & \widehat{D}_{bdI} \\ \hat{D}_{Ibd} & \widehat{D}_{II} \end{bmatrix} \begin{pmatrix} q_{bd} \\ q_I \end{pmatrix} = \begin{pmatrix} f_{bd} \\ f_I \end{pmatrix} \tag{D.2}$$

Considering no external forces applied on the cells internal DOFs such that $f_I = 0$ then

$$\begin{bmatrix} \widehat{D}_{bdbd} & \widehat{D}_{bdI} \\ \widehat{D}_{Ibd} & \widehat{D}_{II} \end{bmatrix} \begin{pmatrix} q_{bd} \\ q_I \end{pmatrix} = \begin{pmatrix} f_{bd} \\ 0 \end{pmatrix} \tag{D.3}$$

The above equation expressed in condensed form as

$$D_{bd} q_{bd} = f_{bd} \tag{D.4}$$

where condensed dynamic stiffness matrix expressed as

$$D_{bd} = \widehat{D}_{bdbd} - \widehat{D}_{bdI} \widehat{D}_{II}^{-1} \widehat{D}_{Ibd} \tag{D.5}$$

Considering uncertainties in the parameters, the dynamic stiffness matrix is uncertain.The stochastic condensed dynamics stiffness matrix written as

$$\widetilde{D}_{bd} = \widetilde{\widehat{D}}_{bdbd} - \widetilde{\widehat{D}}_{bdI} \widetilde{\widehat{D}}_{II}^{-1} \widetilde{\widehat{D}}_{Ibd} \tag{D.6}$$

where symbol $\widetilde{\widehat{(.)}}$ represents the stochastic entity from the original dynamic stiffness matrix. The first order expansion of the above equation leads to

$$\sigma_{D_{bd}} = \sigma_{\widehat{D}_{bdbd}} - \overline{\widehat{D}}_{bdI} \overline{\widehat{D}}_{II}^{-1} \sigma_{\widehat{D}_{Ibd}} + \overline{\widehat{D}}_{bdI} \overline{\widehat{D}}_{II}^{-2} \sigma_{\widehat{D}_{II}} \overline{\widehat{D}}_{Ibd} - \sigma_{\widehat{D}_{bdI}} \overline{\widehat{D}}_{II}^{-1} \overline{\widehat{D}}_{Ibd} \tag{D.7}$$

This can also be expressed as

$$\sigma_{D_{bd}} = \sigma_{\widehat{D}_{bdbd}} - \overline{\widehat{D}}_{bdI} \overline{\widehat{D}}_{II}^{-1} \sigma_{\widehat{D}_{Ibd}} + \overline{\widehat{D}}_{bdI} \overline{\widehat{D}}_{II}^{-1} \sigma_{\widehat{D}_{II}} \overline{\widehat{D}}_{II}^{-1} \overline{\widehat{D}}_{Ibd} - \sigma_{\widehat{D}_{bdI}} \overline{\widehat{D}}_{II}^{-1} \overline{\widehat{D}}_{Ibd} \tag{D.8}$$

Above expression can be expressed in the matrix form and the standard deviation of the condensed dynamic stiffness matrix is

$$\sigma_{D_{bd}} = \left[ \sigma_{\widehat{D}_{bdbd}} \right] - \left[ \overline{\widehat{D}}_{bdI} \quad \sigma_{\widehat{D}_{bdI}} \right] \begin{bmatrix} \overline{\widehat{D}}_{II}^{-1} & -\overline{\widehat{D}}_{II}^{-1} \sigma_{\widehat{D}_{II}} \overline{\widehat{D}}_{II}^{-1} \\ 0 & \overline{\widehat{D}}_{II}^{-1} \end{bmatrix} \begin{bmatrix} \sigma_{\widehat{D}_{Ibd}} \\ \overline{\widehat{D}}_{Ibd} \end{bmatrix} \tag{D.9}$$

where symbol $\overline{\widehat{(.)}}$ represents the mean value from the original dynamic stiffness matrix.

## E. Stochastic wave finite element method (Transfer Matrix) reminder

In one dimensional periodic structure, the nodes on boundary of the periodic structure is denoted as on left boundary ($L$), right boundary ($R$) and remaining/internal nodes ($I$). The displacement degrees of freedom (DOF) $q$ are partitioned into the left ($q_L$) and right ($q_R$). Similarly, forces are partitioned into the left ($F_L$) and right ($F_R$). To accommodate the uncertainties effects random field is considered as a supplementary dimension through the spatial discretisation employing the finite element steps by discretization of one sub-element of length ($d$). The discretisation leads to stochastic dynamic equilibrium of any substructure in following manner

$$(\widetilde{D}) \begin{pmatrix} \widetilde{q}_L^k \\ \widetilde{q}_R^k \end{pmatrix} = \begin{pmatrix} \widetilde{F}_L^k \\ \widetilde{F}_R^k \end{pmatrix} \tag{E.1}$$

where $(\widetilde{D})$ is the stochastic complex dynamic stiffness matrix of the substructure, condensed on left and right boundaries degree of freedom at the pulsation $\omega$

$$(\widetilde{D}) = -\omega^2 \widetilde{M} + \widetilde{K}(1 + i\eta) \tag{E.2}$$

where $\widetilde{M}$, $\widetilde{K}$ are the stochastic mass and the stiffness matrix respectively, $\eta$ is the structural loss factor and $i$ is the unit imaginary number.

In the probabilistic tools, the parametric approach allows considering the uncertainties parameters (material, geometrical properties, etc.) as random quantities. The random variables are modelled using the first order perturbation, as Gaussian variables, such that the dynamical equilibrium is expressed as

$$\left[-\omega^2\left(\overline{M} + \sigma_M\varepsilon\right) + \left(\overline{K} + \sigma_K\varepsilon\right)(1 + i\eta)\right]\begin{pmatrix} \overline{q}_L^{(k)} + \sigma_{q_L}^{(k)}\varepsilon \\ \overline{q}_R^{(k)} + \sigma_{q_R}^{(k)}\varepsilon \end{pmatrix} = \begin{pmatrix} \overline{F}_L^{(k)} + \sigma_F^{(k)}\varepsilon \\ \overline{F}_R^{(k)} + \sigma_F^{(k)}\varepsilon \end{pmatrix} \tag{E.3}$$

The $\overline{(\,)}$ symbol denotes the mean value of the random variable, $\sigma$ is the standard deviation and $\varepsilon$ is a Gaussian centered variable. In the expression $\overline{M}$, $\overline{K}$, $\overline{q}$, $\overline{F}$ are mean quantities of the mass matrix, the stiffness matrix, the displacements vector and the load vector; and $\sigma_M$, $\sigma_K$, $\sigma_q$, $\sigma_F$ are their respective standard deviation. The stochastic problem in Eq. (E.1) can be partitioned in the following way

$$\begin{pmatrix} \widetilde{D}_{LL} & \widetilde{D}_{LR} \\ \widetilde{D}_{RL} & \widetilde{D}_{RR} \end{pmatrix}\begin{pmatrix} \tilde{q}_L^k \\ \tilde{q}_R^k \end{pmatrix} = \begin{pmatrix} \tilde{F}_L^k \\ \tilde{F}_R^k \end{pmatrix} \tag{E.4}$$

Using polynomial chaos projection of the variable in the Eq. (E.4), their mean value and standard deviation can be expressed in following form

$$\begin{pmatrix} \overline{D}_{LL} + \sigma_{D_{LL}}\varepsilon & \overline{D}_{LR} + \sigma_{D_{LR}}\varepsilon \\ \overline{D}_{RL} + \sigma_{D_{RL}}\varepsilon & \overline{D}_{RR} + \sigma_{D_{RR}}\varepsilon \end{pmatrix}\begin{pmatrix} \overline{q}_L + \sigma_{q_L}\varepsilon \\ \overline{q}_R + \sigma_{q_R}\varepsilon \end{pmatrix} = \begin{pmatrix} \overline{F}_L + \sigma_{F_L}\varepsilon \\ \overline{F}_R + \sigma_{F_R}\varepsilon \end{pmatrix} \tag{E.5}$$

In the above expression $\overline{D}$,$\overline{q}$,and $\overline{F}$ are the mean quantities of the dynamic operators, the displacement vectors and the loads respectively; and $\sigma_D$,$\sigma_q$,$\sigma_F$ are their standard deviations. It is to be noted that Eq. (E.5) is valid and can accommodate the stochastic behavior of the stiffness and mass matrices.

The stochastic kinematic variables, $\widetilde{q}$,and $\widetilde{F}$ are represented through stochastic state vectors as $\widetilde{u}_L = \left(\widetilde{q}_L^T \;\; -\widetilde{F}_L^T\right)^T$ and $\widetilde{u}_R = \left(\widetilde{q}_R^T \;\; \widetilde{F}_R^T\right)^T$ ;and related by the stochastic transfer matrix $\tilde{S}$.

$$\widetilde{u}_R^k = \tilde{S}.\tilde{u}_L^k \tag{E.6}$$

Alternatively

$$\begin{pmatrix} \overline{q}_R + \sigma_{q_R}\varepsilon \\ \overline{F}_R + \sigma_{F_R}\varepsilon \end{pmatrix} = \begin{pmatrix} \overline{S}_{LL} + \sigma_{S_{LL}}\varepsilon & \overline{S}_{LR} + \sigma_{S_{LR}}\varepsilon \\ \overline{S}_{RL} + \sigma_{S_{RL}}\varepsilon & \overline{S}_{RR} + \sigma_{S_{RR}}\varepsilon \end{pmatrix}\begin{pmatrix} \overline{q}_L + \sigma_{q_L}\varepsilon \\ -\overline{F}_L - \sigma_F\varepsilon \end{pmatrix} \tag{E.7}$$

The zeroth order expansion of the Eq. (E.7) leads to

$$\begin{pmatrix} \overline{q}_R \\ \overline{F}_R \end{pmatrix} = \begin{pmatrix} \overline{S}_{LL} & \overline{S}_{LR} \\ \overline{S}_{RL} & \overline{S}_{RR} \end{pmatrix}\begin{pmatrix} \overline{q}_L \\ -\overline{F}_L \end{pmatrix} \tag{E.8}$$

Similarly, the zeroth order development of the Eq. (E.5) leads to the following

$$\begin{pmatrix} \overline{F}_L \\ \overline{F}_R \end{pmatrix} = \begin{pmatrix} \overline{D}_{LL} & \overline{D}_{LR} \\ \overline{D}_{RL} & \overline{D}_{RR} \end{pmatrix} \begin{pmatrix} \overline{q}_R \\ \overline{q}_R \end{pmatrix} \tag{E.9}$$

The expansion of Eq. (E.9) leads to

$$\begin{pmatrix} \overline{q}_R \\ \overline{F}_R \end{pmatrix} = -\begin{pmatrix} \overline{D}_{LR} & 0 \\ \overline{D}_{RR} & -1 \end{pmatrix}^{-1} \begin{pmatrix} \overline{D}_{LL} & 1 \\ \overline{D}_{RL} & 0 \end{pmatrix} \begin{pmatrix} \overline{q}_L \\ -\overline{F}_L \end{pmatrix} \tag{E.10}$$

Eq. (E.8) and Eq. (E.10) has similarity and can be written as

$$\begin{pmatrix} \overline{S}_{LL} & \overline{S}_{LR} \\ \overline{S}_{RL} & \overline{S}_{RR} \end{pmatrix} = -\begin{pmatrix} \overline{D}_{LR} & 0 \\ \overline{D}_{RR} & 1 \end{pmatrix}^{-1} \begin{pmatrix} \overline{D}_{LL} & 1 \\ \overline{D}_{RL} & 0 \end{pmatrix}$$

$$\overline{S} = \begin{pmatrix} -\overline{D}_{LR}{}^{-1}\overline{D}_{LL} & -\overline{D}_{LR}{}^{-1} \\ \overline{D}_{RL} - \overline{D}_{RR}\overline{D}_{LR}{}^{-1}\overline{D}_{LL} & -\overline{D}_{RR}\overline{D}_{LR}{}^{-1} \end{pmatrix} \tag{E.11}$$

Similarly, the first order development of the Eq. (E.7) leads to

$$\begin{pmatrix} \sigma_{q_R} \\ \sigma_{F_R} \end{pmatrix} = \begin{pmatrix} \overline{S}_{LL} & \overline{S}_{LR} \\ \overline{S}_{RL} & \overline{S}_{RR} \end{pmatrix} \begin{pmatrix} \sigma_{q_L} \\ -\sigma_{F_L} \end{pmatrix} + \begin{pmatrix} \sigma_{S_{LL}} & \sigma_{S_{LR}} \\ \sigma_{S_{RL}} & \sigma_{S_{RR}} \end{pmatrix} \begin{pmatrix} \overline{q}_L \\ -\overline{F}_L \end{pmatrix} \tag{E.12}$$

The expansion of the Eq. (E.12) leads to

$$\begin{pmatrix} \overline{D}_{LR} & 0 \\ \overline{D}_{RR} & -1 \end{pmatrix} \begin{pmatrix} \sigma_{q_R} \\ \sigma_{F_R} \end{pmatrix} + \begin{pmatrix} \overline{D}_{LL} & 1 \\ \overline{D}_{RL} & 0 \end{pmatrix} \begin{pmatrix} \sigma_{q_L} \\ -\sigma_{F_L} \end{pmatrix} + \begin{pmatrix} \sigma_{D_{LL}} & 0 \\ \sigma_{D_{RL}} & 0 \end{pmatrix} \begin{pmatrix} \overline{q}_L \\ -\overline{F}_L \end{pmatrix} + \begin{pmatrix} \sigma_{D_{LR}} & 0 \\ \sigma_{D_{RR}} & 0 \end{pmatrix} \begin{pmatrix} \overline{q}_R \\ \overline{F}_R \end{pmatrix} = 0 \tag{E.13}$$

Introducing $\begin{pmatrix} \overline{q}_R \\ \overline{F}_R \end{pmatrix}$ from Eq. (E.8), above equation leads to

$$\begin{pmatrix} \overline{D}_{LR} & 0 \\ \overline{D}_{RR} & -1 \end{pmatrix} \begin{pmatrix} \sigma_{q_R} \\ \sigma_{F_R} \end{pmatrix} = -\begin{pmatrix} \overline{D}_{LL} & 1 \\ \overline{D}_{RL} & 0 \end{pmatrix} \begin{pmatrix} \sigma_{q_L} \\ -\sigma_{F_L} \end{pmatrix} - \left[ \begin{pmatrix} \sigma_{D_{LL}} & 0 \\ \sigma_{D_{RL}} & 0 \end{pmatrix} + \begin{pmatrix} \sigma_{D_{LR}} & 0 \\ \sigma_{D_{RR}} & 0 \end{pmatrix} \begin{pmatrix} \overline{S}_{LL} & \overline{S}_{LR} \\ \overline{S}_{RL} & \overline{S}_{RR} \end{pmatrix} \right] \begin{pmatrix} \overline{q}_L \\ -\overline{F}_L \end{pmatrix} \tag{E.14}$$

The simplification of Eq. (E.14), the standard deviation of the stochastic left state vector expressed as

$$\begin{aligned} \begin{pmatrix} \sigma_{q_R} \\ \sigma_{F_R} \end{pmatrix} = -\begin{pmatrix} \overline{D}_{LR} & 0 \\ \overline{D}_{RR} & -1 \end{pmatrix}^{-1} \begin{pmatrix} \overline{D}_{LL} & 1 \\ \overline{D}_{RL} & 0 \end{pmatrix} \begin{pmatrix} \sigma_{q_L} \\ -\sigma_{F_L} \end{pmatrix} - \begin{pmatrix} \overline{D}_{LR} & 0 \\ \overline{D}_{RR} & -1 \end{pmatrix}^{-1} \left[ \begin{pmatrix} \sigma_{D_{LL}} & 0 \\ \sigma_{D_{RL}} & 0 \end{pmatrix} \right. \\ \left. + \begin{pmatrix} \sigma_{D_{LR}} & 0 \\ \sigma_{D_{RR}} & 0 \end{pmatrix} \begin{pmatrix} \overline{S}_{LL} & \overline{S}_{LR} \\ \overline{S}_{RL} & \overline{S}_{RR} \end{pmatrix} \right] \begin{pmatrix} \overline{q}_L \\ -\overline{F}_L \end{pmatrix} \end{aligned} \tag{E.15}$$

Eq. (E.15) represents the standard deviation of the stochastic left state vectors of Eq. (E.5), similarly Eq. (E.12) represents the standard deviation of the stochastic left state vectors of Eq. (E.7). Here comparison of Eq. (E.15) and Eq. (E.12), and identification of $\sigma_S$, leads to write

$$\begin{pmatrix} \sigma_{S_{LL}} & \sigma_{S_{LR}} \\ \sigma_{S_{RL}} & \sigma_{S_{RR}} \end{pmatrix} = -\begin{pmatrix} \overline{D}_{LR} & 0 \\ \overline{D}_{RR} & -1 \end{pmatrix}^{-1} \left[ \begin{pmatrix} \sigma_{D_{LL}} & 0 \\ \sigma_{D_{RL}} & 0 \end{pmatrix} + \begin{pmatrix} \sigma_{D_{LR}} & 0 \\ \sigma_{D_{RR}} & 0 \end{pmatrix} \begin{pmatrix} \overline{S}_{LL} & \overline{S}_{LR} \\ \overline{S}_{RL} & \overline{S}_{RR} \end{pmatrix} \right] \tag{E.16}$$

Introducing $\overline{S}$ from Eq. (E.11) in the above equation leads to

$$\begin{pmatrix} \sigma_{S_{LL}} & \sigma_{S_{LR}} \\ \sigma_{S_{RR}} & \sigma_{S_{RR}} \end{pmatrix} = -\begin{pmatrix} \overline{D}_{LR} & 0 \\ \overline{D}_{RR} & -1 \end{pmatrix}^{-1} \left[ \begin{pmatrix} \sigma_{D_{DL}} & 0 \\ \sigma_{D_{RL}} & 0 \end{pmatrix} + \begin{pmatrix} \sigma_{D_{LR}} & 0 \\ \sigma_{D_{RR}} & 0 \end{pmatrix} \right] \begin{pmatrix} -\overline{D}_{LR}{}^{-1}\overline{D}_{LL} & -\overline{D}_{LR}{}^{-1} \\ \overline{D}_{RL} - \overline{D}_{RR}\overline{D}_{LR}{}^{-1}\overline{D}_{LL} & -\overline{D}_{RR}\overline{D}_{LR}{}^{-1} \end{pmatrix} \tag{E.17}$$

Then the standard deviation of stochastic transfer matrix is

$$\sigma_S = \begin{pmatrix} -\overline{D}_{LR} & 0 \\ -\overline{D}_{RR} & 1 \end{pmatrix}^{-1} \begin{pmatrix} \sigma_{D_{LL}} & \sigma_{D_{LR}} \\ \sigma_{D_{RL}} & \sigma_{D_{RR}} \end{pmatrix} \begin{pmatrix} 1 & 0 \\ -\overline{D}_{LR}{}^{-1}\overline{D}_{LL} & -\overline{D}_{LR}{}^{-1} \end{pmatrix} \tag{E.18}$$

Eq. (E.18) is only valid for the single cell, in case of complex geometry, the internal degree of freedom can be removed using dynamic condensation. The expression for the standard deviation of the condensed dynamic stiffness matrix derived in Appendix B. Following the steps of the deterministic development, a stochastic eigenvalue problem formulated as

$$\begin{aligned} \widetilde{S}\widetilde{\phi}_i &= \widetilde{\mu}_i\widetilde{\phi}_i \\ \left|\widetilde{S} - \widetilde{\mu}_i I_{2n}\right| &= 0 \end{aligned} \tag{E.19}$$

where $\left(\widetilde{\mu}_i, \widetilde{\phi}_i\right)_{i=1\ldots2n}$ are the stochastic waveguide propagation modes. Then stochastic eigensolutions of Eq. (E.19) are expressed as follows

$$\begin{aligned} \widetilde{\mu}_i &= \left(\overline{\mu}_i + \sigma_{\mu_i}\varepsilon\right) \\ \widetilde{\phi}_i &= \left(\overline{\phi}_i + \sigma_{\phi_i}\varepsilon\right) \end{aligned} \tag{E.20}$$

The stochastic eigenvalues are associated to eigenvectors. Then the zeroth order expansion leads to

$$\left(\overline{S} - \overline{\mu}_i I_{2n}\right)\overline{\phi}_i = 0 \tag{E.21}$$

Similarly, the first order expansion of Eq. (E.19) leads to

$$\left(\overline{S} - \overline{\mu}_i I_{2n}\right)\sigma_{\phi_i} + \left(\sigma_s - \sigma_{\mu_i} I_{2n}\right)\overline{\phi}_i = 0 \tag{E.22}$$

In order to extract the first order perturbation of eigenvalues and eigenvectors, use the left propagation constants. Here $\widetilde{\phi}_i^T J_n$ is a left eigenvector of $\widetilde{S}$ which is associated to the eigenvalue $\frac{1}{\widetilde{\mu}_i}$. where

$$J_n = \begin{pmatrix} 0 & I_n \\ -I_n & 0 \end{pmatrix} \tag{E.23}$$

The left stochastic eigenvalue problem can be established as

$$\left(\widetilde{\phi}_i^T J_n\right)\widetilde{S} = \frac{1}{\widetilde{\mu}_i}\left(\widetilde{\phi}_i^T J_n\right) \tag{E.24}$$

The first order expansion of Eq. (E.24) leads to

$$\left(\sigma_{\phi_i}\right)^T J_n\left(\overline{S} - \frac{1}{\overline{\mu}_i} I_{2n}\right) + \overline{\phi}_i^T J_n\left(\sigma_S + \frac{1}{\overline{\mu}_i^2}\sigma_{\mu_i} I_{2n}\right) = 0 \tag{E.25}$$

Simplification of Eq. (E.22) and Eq. (E.25) leads to standard deviation of eigenvalues $\left(\sigma_{\mu_i}\right)$ as

$$\begin{aligned}\sigma_{\mu_i} = &\left[\left(\overline{\phi}_i\right)^T \sigma_S^T \left(\overline{S}^T - \overline{\mu}_i I_{2n}\right)^{-1} J_n \left(\overline{S} - \left(\tfrac{1}{\overline{\mu}_i} I_{2n}\right) - \left(\overline{\phi}_i\right)^T J_n \sigma_S\right)\right] \\ &\left[\left(\overline{\phi}_i\right)^T \left(\overline{S}^T - \overline{\mu}_i I_{2n}\right)^{-1} J_n \left(\overline{S} - (\overline{\mu}_i)^{-1} I_{2n}\right) - \tfrac{1}{\overline{\mu}_i^2} \left(\overline{\phi}_i\right)^T J_n\right]^+\end{aligned} \tag{E.26}$$

Similarly, the standard deviation of the eigenvectors $\left(\sigma_{\phi_i}\right)$ is

$$\sigma_{\phi_i} = -\left[\overline{S} - \overline{\mu}_i I_{2n}\right]^+ \left[\sigma_S - \sigma_{\mu_i} I_{2n}\right] \overline{\phi}_i \tag{E.27}$$

where + is pseudo inverse

Using Eq. (E.26) and Eq. (E.27), the statistics of the wave characteristics can be expressed using the standard deviation of the propagation constants.

Let us consider statistics of the wavenumber expressed as

$$\widetilde{k} = \left(\frac{i}{d}\right) \log \widetilde{\mu} \tag{E.28}$$

where stochastic wave number expressed $\widetilde{k} = \overline{k} + \sigma_k \varepsilon$.

Once the zeroth and first order terms of the stochastic eigenvalue computed, then we can use the statistics of $k$ from Eq. (E.28) to find mean value and dispersion from the mean value. The mean of the wavenumber expressed as

$$\overline{k} = \left(\frac{i}{d}\right) \log(\overline{\mu}) \tag{E.29}$$

Similarly, the dispersion of the wavenumber from the mean can be expressed as

$$\sigma_k = \left(\frac{i}{d}\right) \frac{\sigma_\mu}{\overline{\mu}} \tag{E.30}$$

where $d$ is substructure length.